eNeuro

Research Article: New Research | Cognition and Behavior

Nucleus Accumbens Microcircuit Underlying D2-MSN-Driven Increase in Motivation

Carina Soares-Cunha[1,2], Bárbara Coimbra[1,2], Ana Verónica Domingues[1,2], Nivaldo Vasconcelos[1,2,3], Nuno Sousa[1,2] and Ana João Rodrigues[1,2]

[1]*Life and Health Sciences Research Institute (ICVS), School of Medicine, University of Minho, Braga, Portugal*
[2]*ICVS/3B's–PT Government Associate Laboratory, Braga/Guimarães, Portugal*
[3]*Departamento De Física, Universidade Federal De Pernambuco, Recife, Pernambuco 50670-901, Brazil*

DOI: 10.1523/ENEURO.0386-18.2018

Received: 15 November 2017

Revised: 23 February 2018

Accepted: 28 February 2018

Published: 19 April 2018

Author Contributions: CS-C designed research, performed research, analysed data and wrote the paper; BC, AVD and NAPV performed research; NS designed research; AJR designed research and wrote the paper.

Funding: FCT/Portugal2020
POCI-01-0145-FEDER-016428

Funding: FCT/Norte 2020
NORTE-01-0145-FEDER-000013

Funding: FCT/FEDER
POCI-01-0145-FEDER-007038

Funding: http://doi.org/10.13039/501100005032Fundação Bial (Bial Foundation)
30/2016

The authors declare no competing financial interests.

CS-C was recipient of a Fundação para a Ciência e Tecnologia (FCT) fellowship (SFRH/BD/51992/2012) and is currently recipient of a post-doctoral fellowship from the Programa de Atividades Conjuntas (PAC), through MEDPERSYST project (POCI-01-0145-FEDER-016428; supported by the Portugal2020 Programme). BC is recipient of a PhD scholarship funded by FCT (SFRH/BD/98675/2013). AJR is a FCT Investigator fellow (IF/00883/2013). NAPV is a recipient of a CNPQ grant (249991/2013-6) and a CAPES grant (88887.131435/2016-00).

This work was developed under the scope of the project NORTE-01-0145-FEDER-000013, supported by the Northern Portugal Regional Operational Programme (NORTE 2020), under the Portugal 2020 Partnership Agreement, through the European Regional Development Fund (FEDER). Part of the work was supported by the Janssen Neuroscience Prize (1st edition) and by a BIAL Grant (30/2016).

This work has been funded by FEDER funds, through the Competitiveness Factors Operational Programme (COMPETE), and by National funds, through the Foundation for Science and Technology (FCT), under the scope of the project POCI-01-0145-FEDER-007038 and of project POCI-01-0145-FEDER-016428.

Correspondence should be addressed to: Ana João Rodrigues, Life and Health Sciences Research Institute (ICVS), School of Medicine, University of Minho, Campus de Gualtar, 4710-057 Braga, Portugal. Telephone number: +351 253 604 929, E-mail: ajrodrigues@med.uminho.pt

Manuscript Title: Nucleus accumbens microcircuit underlying D2-MSN-driven increase in motivation

Abbreviated Title: Exploring D2-MSN-dependent increase in motivation

Author Names:

Soares-Cunha C[1,2], Coimbra B[1,2], Domingues AV[1,2], Vasconcelos N[1,2,3], Sousa N[1,2], Rodrigues AJ[1,2*]

Affiliations:

[1]Life and Health Sciences Research Institute (ICVS), School of Medicine, University of Minho, Braga, Portugal

[2]ICVS/3B's–PT Government Associate Laboratory, Braga/Guimarães, Portugal

[3]Departamento de Física, Universidade Federal de Pernambuco, 50670-901 Recife, Pernambuco, Brazil

Author Contributions:

CS-C designed research, performed research, analysed data and wrote the paper; BC, AVD and NAPV performed research; NS designed research; AJR designed research and wrote the paper.

Correspondence should be addressed to:

Name: Ana João Rodrigues

Postal address: Life and Health Sciences Research Institute (ICVS)
School of Medicine, University of Minho
Campus de Gualtar
4710-057 Braga, Portugal

Telephone number: +351 253 604 929

e-mail: ajrodrigues@med.uminho.pt

Number of Figures: 5

Number of Tables: 1 Table

Number of Multimedia: 0 multimedia

Number of words for Abstract: 216 words

Number of words for Significance Statement: 80 words

Number of words for Introduction: 513 words

Number of words for Discussion: 1273 words

Acknowledgements:

A special acknowledgement to Karl Deisseroth from Stanford University, for providing viral constructs. We would like to acknowledge Rui Costa and Ana Vaz from Champalimaud Foundation and Patrícia Monteiro from University of Minho for providing animals and samples for antibody specificity analysis.

Conflict of Interest:

Authors report no conflict of interest.

Funding sources:

CS-C was recipient of a Fundação para a Ciência e Tecnologia (FCT) fellowship (SFRH/BD/51992/2012) and is currently recipient of a post-doctoral fellowship from the Programa de Atividades Conjuntas (PAC), through MEDPERSYST project (POCI-01-0145-FEDER-016428; supported by the Portugal2020 Programme). BC is recipient of a PhD scholarship funded by FCT (SFRH/BD/98675/2013). AJR is a FCT Investigator fellow (IF/00883/2013). NAPV is a recipient of a CNPQ grant (249991/2013-6) and a CAPES grant (88887.131435/2016-00).

This work was developed under the scope of the project NORTE-01-0145-FEDER-000013, supported by the Northern Portugal Regional Operational Programme (NORTE 2020), under the Portugal 2020 Partnership Agreement, through the European Regional Development Fund (FEDER). Part of the work was supported by the Janssen Neuroscience Prize (1st edition) and by a BIAL Grant (30/2016).

This work has been funded by FEDER funds, through the Competitiveness Factors Operational Programme (COMPETE), and by National funds, through the Foundation for Science and Technology (FCT), under the scope of the project POCI-01-0145-FEDER-007038 and of project POCI-01-0145-FEDER-016428.

66 **Title: Nucleus accumbens microcircuit underlying D2-MSN-driven increase in**
67 **motivation**
68
69 **Abbreviated title: Exploring D2-MSN-dependent increase in motivation**
70
71 **Abstract**

72 The nucleus accumbens (NAc) plays a central role in reinforcement and motivation.
73 Around 95% of the NAc neurons are medium spiny neurons (MSNs), divided into those
74 expressing dopamine receptor D1 (D1R) or dopamine receptor D2 (D2R). Optogenetic
75 activation of D2-MSNs increased motivation, whereas inhibition of these neurons produced
76 the opposite effect. Yet, it is still unclear how activation of D2-MSNs affects other local
77 neurons/interneurons or input terminals, and how this contributes for motivation
78 enhancement. To answer this question, in this work we combined optogenetic modulation of
79 D2-MSNs with *in loco* pharmacological delivery of specific neurotransmitter antagonists in
80 rats.
81 First, we showed that optogenetic activation of D2-MSNs increases motivation in a
82 progressive ratio task. We demonstrated that this behavioural effect relies on cholinergic-
83 dependent modulation of dopaminergic signalling of ventral tegmental area (VTA) terminals,
84 which requires D1R and D2R signalling in the NAc. D2-MSN optogenetic activation
85 decreased ventral pallidum (VP) activity, reducing the inhibitory tone to VTA, leading to
86 increased dopaminergic activity. Importantly, optogenetic activation of D2-MSN terminals in
87 the VP was sufficient to recapitulate the motivation enhancement.
88 In summary, our data suggests that optogenetic stimulation of NAc D2-MSNs indirectly
89 modulates VTA dopaminergic activity, contributing for increased motivation. Moreover, both
90 types of dopamine receptors signalling in the NAc are required in order to produce the
91 positive behavioural effects.
92

Significance statement

The nucleus accumbens (NAc) is a key brain region of the reward system and is crucial for motivation. We showed that activation of NAc D2-expressing neurons enhances motivation by modulating VTA dopaminergic activity via ventral pallidum inhibition. The behavioural effect was dependent on local cholinergic-dependent dopamine release by VTA terminals that required D1 and D2 dopamine receptors in the NAc.

This study reveals for the first time how D2-MSN stimulation can modulate downstream regions and local microcircuit to increase motivation.

Introduction

Dopaminergic projections from the ventral tegmental area (VTA) to the nucleus accumbens (NAc) have been classically described as the core of the reward circuit (Wise, 2004). Evidence in animal models and humans showed that the motivational aspects of reward processing are greatly mediated by these projections (Bailey et al., 2016; Hyman et al., 2006; Kelley and Berridge, 2002; Wise, 1998). The NAc contains 95% of medium spiny neurons (MSNs), that are typically divided into those that express dopamine receptor D1 (D1R, D1-MSNs), and those that express dopamine receptor D2 (D2R, D2-MSNs). In addition to dopaminergic inputs from the VTA, these MSNs receive dense monosynaptic glutamatergic innervation from the medial prefrontal cortex, hippocampus and amygdala (Haber, 2003). These MSNs project directly to the VTA through the direct pathway, mediated exclusively by D1-MSNs, or indirectly via the ventral pallidum (VP) (both D1- and D2-MSNs) (Kupchik et al., 2015; Lu et al., 1998; Zhou et al., 2003). Additionally, MSNs are known to synapse within each other (Dobbs et al., 2016; Sesack and Pickel, 1990), maintaining GABAergic accumbal activity under a balanced control.

The remaining 5% of NAc neurons are local interneurons, that include large tonically active cholinergic interneurons (CIN), fast spiking (FS) GABAergic interneurons, low threshold spiking (LTS) interneurons (Soares-Cunha et al., 2016b), as well as less explored

subtypes, namely tyrosine hydroxylase interneurons (Ibáñez-Sandoval et al., 2015, 2010) and calretinin interneurons (Tepper and Bolam, 2004). Importantly, both cholinergic and GABAergic interneurons play a crucial role in NAc activity and response to salient stimuli and modulate reward-dependent behaviors (Lim et al., 2014; Tepper and Bolam, 2004).

In the past years, compelling data supported a role for D1-MSNs in positive reinforcement, while D2-MSNs have been mostly associated with aversion. Nonetheless, recent data emerged in opposition to this dichotomy; whereas the division of direct and indirect neurons based on the respective expression of D1R and D2R in dorsal striatum appears to be precise, in the NAc the indirect pathway contains a mixture of D1-MSNs and D2-MSNs (Kravitz et al., 2012; Lobo et al., 2010). This implies that both NAc D1- and D2-MSNs can inhibit or disinhibit thalamic activity, with clear repercussions in behavior. In agreement with this view, a previous study showed that activation of either NAc D1- or D2-MSNs is sufficient to increase motivation in a progressive ratio task (PR) (Soares-Cunha et al., 2016a). In the same direction, in the ventrolateral striatum, both D1- and D2-MSNs are activated at the trial start cue in the PR test and inhibition of either population immediately after the cue resulted in decreased motivation (Natsubori et al., 2017).

These seminal findings showed that D2-MSNs play a more pro-motivation/reward role than initially anticipated, and suggest that the prevailing notion of a functional segregation of MSNs should be reconsidered. Yet, it is still unclear how activation of D2-MSNs affects other local neurons/interneurons and downstream regions and how this contributes for motivation enhancement. Therefore, we combined optogenetic activation of NAc D2-MSNs with *in loco* pharmacological delivery of specific antagonists in order to identify the contribution of different NAc inputs and neuronal populations for motivational drive.

Materials and methods

Animals

Male Wistar Han rats (2-3 months old at the beginning of the tests) were used. Animals were maintained under standard laboratory conditions: 12h light/dark cycle (lights on from

8am to 8pm) and room temperature of 21±1°C, with relative humidity of 50-60%; rats were individually housed after optical fibre implantation; standard diet (4RF21, Mucedola SRL) and water were given *ad libitum*, until the beginning of the behavioural experiments, in which animals switched to food restriction to maintain 85% of initial body weight.

Behavioural manipulations occurred during the light period of the light/dark cycle. Health monitoring was performed according to FELASA guidelines (Nicklas et al., 2002). All procedures were conducted in accordance with European Regulations (European Union Directive 2010/63/EU). Animal facilities and animals' experimenters were certified by the National regulatory entity – DGAV. All protocols were approved by the Ethics Committee of the ICVS and by DGAV.

Experimental Design

Group I of animals ($n_{D2\text{-}ChR2}$=10, $n_{D2\text{-}eYFP}$=7), that received intracranial viral injection and optical fiber placement in the NAc, performed the progressive ratio test (described below) and were sacrificed 90 minutes after the beginning of the last PR session for c-fos analysis (Fig. 1-1A).

Group II of animals ($n_{D2\text{-}ChR2}$=8, $n_{D2\text{-}eYFP}$=7), that received intracranial viral injection and hybrid cannula (optics and fluid) placement in the NAc, performed the progressive ratio test (described below) and performed two additional PR sessions with antagonist injections. On day 1, half of the animals received antagonist injection and the other half received vehicle injection. On day two, animals receiving drug on the first day received vehicle and vice versa. All animals were treated with vehicle and drug. After behavioral performance, all rats were sacrificed, and cannula placement and viral expression were confirmed (Fig. 1-1B).

Group III of animals ($n_{D2\text{-}ChR2\ NAc\text{-}VP}$=8, $n_{D2\text{-}eYFP\ NAc\text{-}VP}$=6), that received intracranial viral injection in the NAc and optical fiber placement in the VP, performed the progressive ratio test (described below) (Fig. 1-1C).

Group IV of animals ($n_{D2\text{-}ChR2}$=4) was injected with ChR2 in the NAc, and after 3 weeks to allow viral expression, *in vivo* single unit electrophysiological recordings were performed

177 (Fig. 1-1D).

178

179 **Behavior**

180 **Subjects and apparatus**

181 Rats were habituated to 45 mg food pellets (F0021; BioServ), which were used as
182 reward during the behavioral protocol, one day prior to training initiation. Behavioral sessions
183 were performed in operant chambers (Med Associates) that contained a central, recessed
184 magazine to provide access to 45mg food pellets (Bio-Serve), two retractable levers with
185 cue lights located above them that were located on each side of the magazine. Chamber
186 illumination was obtained through a 2.8W, 100mA light positioned at the top-center of the
187 wall opposite to the magazine. The chambers were controlled by a computer equipped with
188 the Med-PC software (Med Associates).

189

190 **Progressive Ratio (PR) schedule of reinforcement**

191 All training sessions started with illumination of the house light that remained until the
192 end of the session. On the first training session (CRF; continuous reinforcement sessions)
193 one lever was extended. The lever would remain extended throughout the session, and a
194 single lever press would deliver a food pellet (maximum of 50 pellets earned within 30min).
195 In some cases, food pellets were placed behind the lever to promote lever pressing. After
196 successful completion of the CRF training, rats were trained to lever press on the opposite
197 lever using the same training procedure. In the 4 following days, the side of the active lever
198 was alternated between sessions. Then, rats were trained to lever press one time for a
199 single food pellet in a fixed ratio (FR) schedule consisting in 50 trials in which both levers are
200 presented, but the active lever is signaled by the illumination of the cue light above it. FR
201 sessions began with extension of both levers (active and inactive) and illumination of the
202 house light and the cue light over the active lever. Completion of the correct number of lever
203 press led to a pellet delivery, retraction of the levers and the cue light turning off for a 20s
204 ITI. Rats were trained first with one lever active and then with the opposite lever active in

205 separate sessions (in the same day). In a similar manner, rats were then trained using an
206 FR4 reinforcement schedule for 4 days and a FR8 for 1 day. On the test day, rats were
207 exposed to PR or FR experimental sessions (one session per day) according to the following
208 schedule: day 1 – FR4; day 2 – PR (Optical stimulation); day 3 – FR4; day 4 – PR (no
209 optical stimulation). PR sessions were identical to FR4 sessions except that the operant
210 requirement on each trial (T) was the integer (rounded down) of $1.4^{(T-1)}$ lever presses,
211 starting at 1 lever press. PR sessions ended after 15 min elapsed without completion of the
212 response requirement in a trial.

213 Before the PR session, rats were connected to an opaque optical fiber, through
214 previously implanted cannula guide placed in the NAc. At the beginning of each trial of the
215 PR session with optical stimulation – when the retractable levers are exposed to the animal
216 together with the cue light – animals received an optical stimulation. After basal assessment
217 of PR (one session with optical stimulation and one session without), all animals performed
218 7 additional sessions (with one week interval and 1 FR4 reminder session prior to PR test)
219 with optical stimulation and local pharmacological administration of receptors antagonist
220 (Fig. 1-1).

221 Optical stimulation was performed as follows: 473nm; frequency of 40Hz; 12.5ms pulses
222 over 1s; 10mW at the tip of the implanted fiber.

223

224 **Constructs and virus preparation**

225 eYFP or hChR2(H134R)-eYFP were cloned under the control of the D2R minimal
226 promoter region as described before (Soares-Cunha et al., 2016a; Zalocusky et al., 2016).
227 Constructs were packaged in AAV5 serotype by the UNC Gene Therapy Center Vector Core
228 (UNC). AAV5 vector titters were $3.7\text{-}6\text{x}10^{12}$ viral molecules/ml as determined by dot blot.

229

230 **Surgery and cannula implantation**

231 Rats were anesthetized with 75mgkg^{-1} ketamine (Imalgene, Merial) plus 0.5 mg kg^{-1}
232 medetomidine (Dorbene, Cymedica). Virus was unilaterally injected into the NAc;

coordinates from bregma, according to (Paxinos and Watson, 2005): +1.2mm anteroposterior (AP), +1.2mm mediolateral (ML), and -6.5mm dorsoventral (DV) (D2-ChR2 group and D2-eYFP control group). Rats that performed the PR with only optical stimulation were implanted with an optic fiber (200µm diameter) attached to a 2.5mm ferrule (Thorlabs), and rats that performed the PR test with both optical stimulation and local administration of antagonists were implanted with opto-fluid cannulas (Doric Lenses) using the injection coordinates (except for the dorsoventral: -6.4mm) that were secured to the skull using 2.4mm screws (Bilaney) and dental cement (C&B kit, Sun Medical).

For NAc terminal stimulation in the VP, virus was injected as above but rats were implanted with an optic fiber in the VP - coordinates from bregma: -0.1mm AP, +2.4mm ML, and -7mm DV (D2-ChR2 NAc-VP group and D2-eYFP NAc-VP control group).

Rats were allowed to recover for two weeks before initiation of the behavioural trainings.

***In vivo* single-cell electrophysiology**

Three weeks post-surgery, D2-ChR2 rats (n=4) were anaesthetized with urethane (1.44gkg^{-1}, Sigma). The total dose was administered in three separate intraperitoneal injections, 15min apart. Adequate anesthesia was confirmed by the lack of withdrawal responses to hindlimb pinching. A recording electrode coupled with a fiber optic patch cable (Thorlabs) was placed in the NAc (coordinates from bregma: +1.2mm AP, +1.2mm ML, and -6.0 to -7.0mm DV), using a stereotaxic frame (David Kopf Instruments) with non-traumatic ear bars (Stoeling). Other recording electrodes with fiber optic attached were placed in the VP (coordinates from bregma: 0 to -0.12mm AP, +2.3 to +2.5mm ML, and -7 to -7.6mm DV) and in the VTA (coordinates from bregma: -5.3mm AP, +0.9mm ML, and -7.5 to -8.3mm DV).

Single neuron activity was recorded extracellularly with a tungsten electrode (tip impedance 5–10 Mat 1kHz) and data sampling was performed using a CED Micro1401 interface and Spike 2 software (Cambridge Electronic Design). The DPSS 473nm laser system, controlled by a stimulator (Master-8, AMPI) was used for intracranial light delivery.

Optical stimulation was performed as follows: 473nm; frequency of 40Hz; 12.5ms pulses over 1s, 10mW.

Firing rate histograms were calculated for the baseline (10s before stimulation), stimulation period and after stimulation period (10s after the end of stimulation). Spike latency was determined by measuring the time between half-peak amplitude for the falling and rising edges of the unfiltered extra-cellular spike.

NAc neurons were classified according to previous descriptions (Jin et al., 2014; Vicente et al., 2016). In short, fast-spiking interneurons – putative parvalbumin-containing neurons (pFSs) – were identified has having a waveform half-width of less that 100μs and a baseline firing rate higher that 10Hz; tonically active putative cholinergic interneurons (pCINs) were identified as those with a waveform half-width bigger that 300μs. Putative MSNs (pMSNs) were identified as those with baseline firing rate lower that 5Hz and that do not met the waveform criteria for pCIN or pFS neurons.

VP GABAergic neurons were identified as those having a baseline firing rate between 0.2 Hz and 18.7 Hz (Richard et al., 2016). Other non-identified neurons (corresponding to less that 5% of recorded cells) were excluded from the analysis.

Single units in the VTA were separated into those putative dopaminergic (pDAergic) and putative GABAergic (pGABAergic). This classification was based on firing rate and waveform duration (Totah et al., 2013; Ungless et al., 2004; Ungless and Grace, 2012). Cells presenting baseline firing rate lower that 10Hz and a waveform duration higher than 1.5ms were considered pDAergic neurons. Cells presenting baseline firing rate higher than 10Hz and waveform duration lower than 1.5ms were classified as pGABAergic. Other single units that did not fit in any classification (less than 5% of recorded cells) were excluded from the analysis.

Immunofluorescence (IF)

Ninety min after initiation of the PR test, rats were deeply anesthetized with pentobarbital (Eutasil) and were transcardially perfused with 0.9% saline followed by 4%

paraformaldehyde. Brains were removed and post-fixed in 4% paraformaldehyde. Coronal vibratome sections (50µm) were incubated with mouse anti-D2R (1:500, CAT#sc-5303, RRID: AB_668816, Santa Cruz Biotechnology); rabbit anti-c-fos (1:1000, Merck Millipore CAT#Ab-5, RRID: AB_2314042), goat or mouse anti-GFP (1:500, Abcam CAT#ab6673, RRID: AB_305643; or Abcam CAT#ab1218, RRID: AB_298911), mouse anti-D1R (1:100, Novus CAT#NB110-60017, RRID: AB_905382) and goat anti-ChAT (1:750, Millipore CAT#AB144P, RRID: AB_2079751). Appropriate secondary fluorescent antibodies were used (1:500, Invitrogen; CAT# A-21206, RRID:AB_141708; CAT# R37119, RRID:AB_2556547; CAT# A-21202, RRID:AB_141607; CAT# R37114, RRID:AB_2556542; CAT# A-11055, RRID:AB_142672). Finally, all sections were stained with 4′,6-diamidino-2-phenylindole (DAPI; 1mgml^{-1}). Anti-D1R and anti-D2R antibodies were previously validated (Basu et al., 2004; Luedtke et al., 1999; Luessen et al., 2016) (Fig. 5-1).

For each brain region, counting's were performed in 5 distinct 50µm sections. Images were collected and analysed by confocal microscopy (Olympus FluoViewTMFV1000). Cell counts were normalized to the area of the brain region.

Drugs

All drugs were delivered 10 minutes before animals performed the PR test, through an opto-fluid system chronically implanted in the NAc. Injections were performed using a 5µL gastight seringe (Hamilton), attached to the implanted injection cannula of the rats through 22-gauge tubing, at a constant rate of 1µL per minute.

The drugs used in experimental procedures were: R(+)-SCH-23390 hydrochloride (D1R antagonist, 0.25µg in 0.5µL of saline, Sigma); (S)-(-)-Sulpiride (D2R antagonist, 0.2µg in 1µL, Sigma); Scopolamine Hydrobromide (mAChR antagonist, 25µg in 1µL, Sigma); Mecamylamine hydrochloride (nAChR antagonist, 22.5µg in 1µL, Sigma); Dihydro-β-erythroidine hydrobromide (DHβE, α4-nAChR antagonist, 0.7µg in 1µL, Tocris); CGP-55845 hydrochloride (GABA(B) receptor antagonist, 44ng in 0.5µL, Sigma); 1(S),9(R)-(-)-Bicuculine methobromide (GABA(A) receptor antagonist, 75ng in 0.5µL, Sigma).

317

318 **Statistical analysis**

319 Normality tests were performed for all data analysed, as well as outlier analysis using
320 Tukey's test. Statistical analysis between two groups was made using two-tailed Student's *t*-
321 test (unpaired *t-test* for comparison between two groups; paired *t-test* for comparison within
322 the same group). One-way or two-way analysis of variance (ANOVA) was used when
323 appropriate. Bonferroni's *post hoc* multiple comparisons were used for group differences
324 determination. Statistical results are displayed in Table 1.

325 Results are presented as mean ± SEM. All statistical analysis was performed using
326 GraphPad Prism (v7.0) and results were considered significant for $p \leq 0.05$.

327

328

329

Results

Optogenetic stimulation of NAc D2-MSNs increases motivation

In order to specifically modulate the activity of nucleus accumbens (NAc) D2R-expressing neurons, we injected in the NAc of rats a construct containing channelrhodopsin (ChR2) in fusion with enhanced yellow fluorescent protein (eYFP) under the control of the D2R minimal promoter (pAAV-D2Rp-hChR2(H134R)-eYFP), or the control eYFP virus (pAAV-D2Rp-eYFP) (Figs. 1A-B; Fig. 1-2) (Soares-Cunha et al., 2016a; Zalocusky et al., 2016). Nearly 60% of NAc D2R-expressing neurons were successfully transfected with ChR2 or eYFP ($D2R^+$/$eYFP^+$ cells; Fig. 1C). In addition, only 1.5% of $eYFP^+$ cells were $D1R^+$; and 2% were $ChAT^+$. Forty % of $ChAT^+$ cells (CINs) were transfected since they express eYFP (Fig. 1-2).

Using single-cell *in vivo* electrophysiology, we showed that D2-MSN optical stimulation (40Hz, 40 light pulses at 12.5ms) significantly increases NAc firing rate during stimulation in comparison with baseline, and 84% of the cells return to basal activity after stimulation (Fig. 1D-F; $F(2,48)=76.7$, $p<0.000$, one-way ANOVA). 68% of recorded cells increased activity, 16% decrease and 24% did not change activity in response to stimulation. Spike latency was ~2ms (Fig. 1G).

After, animals were submitted to PR test (Fig. 1-1) to evaluate their willingness to work for a food reward, a direct measure of individual motivation. During continuous reinforcement (CRF) training, both groups increased lever pressing throughout days in a similar manner (Fig. 1H; $F(1,15)=0.43$, $p=0.522$, 2way ANOVA). Likewise, all animals increased lever pressing in the fixed-ratio (FR) schedule days in the active vs non-active lever (Fig. 1I; $F(3,30)=126.8$, $p<0.000$, 2way ANOVA).

In agreement with previous findings (Soares-Cunha et al., 2016a), D2-MSN optical stimulation (40 light pulses of 12.5ms at 40Hz) occurring at the same time as the conditioned stimulus (light above the active lever), induced a significant increase in the breakpoint of D2-ChR2 rats in comparison with D2-eYFP stimulated rats (63.6% increase; Fig. 1J; $t(15)=7.7$, $p<0.000$, unpaired *t-test*). All D2-ChR2 rats displayed a significant increase in the breakpoint

in the session with optical stimulation (ON) in comparison with the session without stimulation (OFF) (Fig. 1K; 2way ANOVA *post hoc* $p<0.000$). This increase in motivation was not due to differences in the number of food pellets earned during the PR session (Fig. 1L; $t(15)=1.5$, $p=0.1380$, unpaired *t-test*). Stimulation occurring during the inter-trial interval (ITI) had no effect on motivation (Fig. 1M-N), proving that the positive effect of stimulation in behavior was restricted to particular stages of the test.

Increase in motivation is dependent on NAc GABA signaling

MSNs are GABAergic in nature and synapse within each other in the NAc (Dobbs et al., 2016). Besides, local interneurons provide an additional source of GABA that also controls MSNs activity (Fig. 2A) (Tepper et al., 2004).

To further understand the impact of GABAergic neurotransmission in the control of D2-MSN-mediated enhancement of motivation, we used hybrid cannulas, which allow dual delivery of drugs and light in the same region (Fig. 1-1; Fig. 2-1). Immediately before behavioral testing and optogenetic activation of D2-MSNs, we injected in the NAc either a $GABA_A$ receptor antagonist (bicuculline, 75ng) or a $GABA_B$ receptor antagonist (CGP 55845 hydrochloride, 44ng), in dosages that have been shown previously to induce a behavioral effect (Giorgetti et al., 2002; Ikeda et al., 2010; Kandov et al., 2006).

For $GABA_A$ receptor antagonist, we found no significant effect of treatment but there was a group effect, with D2-ChR2 stimulated animals presenting increased breakpoint (Fig. 2B; 2way ANOVA; treatment effect: $F(1,13)=0.1$, $p=0.117$; group effect: $F(1,13)=118.8$, $p<0.000$). For $GABA_B$ receptor antagonist, there was a significant effect of treatment and group (Fig. 2C; 2way ANOVA; treatment effect: $F(1,13)=30.7$, $p<0.000$; group effect: $F(1,13)=193$, $p<0.000$).

None of the GABA antagonists alters the breakpoint of control D2-eYFP animals (Fig. 2B-C), though there was a trend for increased number of lever presses with $GABA_B$ receptor antagonist treatment (12% increase; $p=0.070$, 2way ANOVA *post hoc*). $GABA_A$ receptor antagonist administration prior to D2-MSN stimulation did not impair the breakpoint

386 enhancement (Fig. 2B; D2-ChR2 vehicle vs D2-ChR2 $GABA_A$ antag, p=0.787, 2way ANOVA
387 *post hoc*). However, administration of $GABA_B$ receptor antagonist led to an additional
388 increase in the breakpoint of D2-stimulated animals (15.8% increase; Fig. 2C; p<0.000,
389 2way ANOVA *post hoc*). No differences were found between groups in the number of pellets
390 earned during the session (Fig. 2-2).
391 These results suggest that GABA signalling arising from MSNs or local interneurons can
392 modulate motivational drive in a $GABA_B$-dependent manner.
393
394 **Increase in motivation is dependent on NAc cholinergic signaling**
395 In addition to GABAergic modulation, MSNs activity is tightly controlled by cholinergic
396 interneurons (CIN) (Fig. 2A), which are able to control dopamine release from VTA terminals
397 in the NAc (Cachope et al., 2012), promoting behavioral conditioning (Witten et al., 2010).
398 Using a similar approach as above, we injected in the NAc a combination of muscarinic
399 (mAChR) and nicotinic acetylcholine receptor (nAChR) antagonists prior to PR paradigm
400 (scopolamine, 25µg; mecamylamine, 22.5µg, respectively; dosages previously validated
401 (Nadal et al., 2002; Perry et al., 2014; Rahman and McBride, 2002; Yee et al., 2011)).
402 Treatment had a significant effect on behavior (Fig. 2D; F(3,39)=6.3, p=0.001, 2way
403 ANOVA). Blockade of cholinergic signalling significantly abolished the motivation
404 enhancement induced by optogenetic D2-MSN activation (Fig. 2D; D2-ChR2 vehicle vs D2-
405 ChR2 mAChR+nAChR antag, p<0.000, 2way ANOVA *post hoc*).
406 Further studies using either one of the antagonists revealed that this blockage was
407 mediated by nAChR (Fig. 2D; D2-ChR2 vehicle vs D2-ChR2 nAChR antag, 2way ANOVA
408 *post hoc*, p<0.000). No differences in the number of pellets earned during the session were
409 found (Fig. 2-2).
410 In the NAc, MSNs express mAChR (M1 and M4) (Yan et al., 2001) but not nAChR
411 (Jones et al., 2001; Jones and Wonnacott, 2004). The later receptors are mainly expressed
412 in VTA dopaminergic terminals (Hill et al., 1993) and some GABAergic interneurons (Koós
413 and Tepper, 1999) (Fig. 2A). Tonic striatal acetylcholine is able to promote dopamine

414 release through beta2-subunit-containing (β2*)-nAChR receptors in VTA terminals (Rice and
415 Cragg, 2004). Using different KO strains, Champtiaux and colleagues proposed that a
416 combination of α6β2* and α4β2* nAChRs mediate the endogenous cholinergic modulation of
417 dopamine release at the terminal level (Champtiaux et al., 2003). Considering this, we
418 injected DHβE (0.7 µg; dosage validated (Löf et al., 2007)), an antagonist of α4 subunit of
419 nAChR, in the NAc before performing the PR test. By blocking α4 receptors, we are
420 abolishing at least 50% of dopamine release in the NAc (Champtiaux et al., 2003).
421 Treatment using α4 antagonist had a significant effect on behavioral performance (Fig.
422 2E; $F(1,13)=43.0$, $p<0.000$, 2way ANOVA). No effect in the breakpoint of control animals
423 was found, yet, this treatment abolished the enhancement of breakpoint induced by D2-MSN
424 stimulation (20.8% decrease; $p<0.000$, 2way ANOVA *post hoc*). No effect on the number of
425 pellets earned during the session was found (Fig. 2-2).
426 These results suggest that cholinergic activation of VTA terminals is required for the
427 observed behavioural effect of D2-MSN stimulation.
428
429 **Enhancement of motivation by D2-MSN activation requires dopamine signaling**
430 **through D1R and D2R**
431 Activating α6β2* and/or α4β2* nAChRs in VTA terminals greatly enhances dopamine
432 release in the NAc (Cachope et al., 2012; Wonnacott et al., 2000), and our previous results
433 suggested that cholinergic modulation of VTA terminals was necessary for the observed
434 motivation enhancement induced by D2-MSN optogenetic activation. Thus, we next tried to
435 clarify the role of NAc dopamine receptors D1R and D2R in this process. To do so, we
436 injected in the NAc before performance of PR test with optogenetic stimulation of D2-MSNs,
437 R(+)-SCH-23390 hydrochloride (0.5 µg; D1R antagonist) or sulpiride (0.2 µg ; D2R
438 antagonist) in doses that were previously shown to have a behavioural effect (Vezina et al.,
439 1994).
440 Both D1R and D2R antagonist treatment had a significant effect (Fig. 2F-G; 2way
441 ANOVA; D1R antag: $F(1,13)=65.7$, $p<0.000$; D2R antag: $F(1,13)=56.8$, $p<0.000$).

Interestingly, both antagonists caused a reduction in the breakpoint of control D2-eYFP animals (D1R antagonist: 25.1% decrease, p=0.047, 2way ANOVA *post hoc*; D2R antagonist: 26.2% decrease, p=0.013, 2way ANOVA *post hoc*).

Additionally, pharmacological inhibition of either D1R or D2R abolished the increase in motivation induced by D2-MSN optogenetic activation (D2-ChR2 vehicle vs D2-ChR2 D1R antag: p<0.000, 2way ANOVA *post hoc*; D2-ChR2 vehicle vs D2-ChR2 D2R antag: p<0.000, 2way ANOVA *post hoc*). A reduction in the number of pellets consumed in D1R-treated D2-eYFP rats was found (Fig. 2-2, p=0.0164, 2way ANOVA *post hoc*). No significant differences in the number of pellets consumed were found in other groups.

These results suggest that the motivation improvement is dependent on both types of dopamine receptor signalling in the NAc.

Optogenetic stimulation of NAc D2-MSNs recruits the VP and the VTA

The preceding results suggested a dopamine-dependent effect of D2-MSN optogenetic activation in motivation (summarized in Fig. 2H). D2-MSNs do not directly project to VTA, but indirectly modulate VTA dopaminergic activity through the ventral pallidum (VP) (Floresco et al., 2003; Grace et al., 2007; Hjelmstad et al., 2013; Kupchik et al., 2015; Wu et al., 1996). So, we next examined the pattern of expression of c-fos, an immediate early gene used as a marker of neuronal recruitment, after the PR test in the NAc and connected regions.

Stimulated D2-ChR2 rats showed a significant increase in c-fos staining in NAc D2R-expressing neurons, when compared with stimulated control D2-eYFP rats (Fig. 3A-B; Fig. 3-1; t(13)=12.0, p<0.000, unpaired *t-test*), and when compared with the non-stimulated side (t(7)=7.4, p=0.0002, paired *t-test*). This increase in c-fos expression was also observed in NAc D1R-expressing neurons when comparing D2-ChR2 with D2-eYFP rats (Figs. 3A, 3C; t(13)=3.7, p=0.0028, unpaired *t-test*), and with the contralateral non-stimulated side (t(7)=5.3, p=0.0011, paired *t-test*).

ChAT-expressing neurons also presented increased c-fos expression when comparing D2-ChR2 with D2-eYFP rats (Figs. 3A, 3D; t(13)=5.7, p<0.000, unpaired *t-test*), or comparing with contralateral non-stimulated side (t(7)=4.0, p=0.0053, paired *t-test*).

In addition, we evaluated the number of c-fos$^+$ cells in accumbal downstream regions: the VTA, which is innervated solely by NAc D1-MSNs (Bocklisch et al., 2013); the VP, which is directly innervated by NAc D1- and D2-MSNs (Creed et al., 2016); and the substantia nigra pars compacta (SNc) as a control region, since it is mainly innervated by dorsal striatum MSNs (Gerfen, 1984).

A significant increase in VTA c-fos$^+$ cells was observed in D2-ChR2 rats in comparison to D2-eYFP stimulated rats (Figs. 3E-F; t(13)=5.3, p<0.000, unpaired *t-test*), or when comparing with contralateral side (t(7)=4.6, p=0.0024, paired *t-test*); from these, around 30% were dopaminergic neurons (t(13)=7.1, p<0.000, unpaired *t-test*). A similar increase in c-fos was observed in the VP of D2-ChR2 in comparison with D2-eYFP rats (Fig. 3H-I; t(13)=2.3, p=0.039, unpaired *t-test*). However, no significant difference in c-fos was found between stimulated and contralateral VP in D2-ChR2 rats (t(7)=1.2, p=0.258, paired *t-test*). D2-MSN accumbal stimulation did not alter c-fos expression in the SN (Fig. 3G).

Optogenetic activation of NAc-VP terminals recapitulates motivation enhancement

Next, we analyzed the activity of the VP and VTA during D2-MSN optogenetic stimulation using *in vivo* single cell electrophysiology (Fig. 4A).

Concordant with a GABAergic input, NAc D2-MSN stimulation elicited an overall reduction in the firing rate of the VP (Fig. 4B; F(2,87)=10.6, p<0.000, one-way ANOVA), with an average spike latency of 5.7ms (Fig. 4-1A), consistent with the expected monosynaptic input from the NAc to VP. More than 90% of recorded neurons in the VP decreased their activity during stimulation, which normalized thereafter (Fig. 4C-D).

Conversely, in the VTA, we found a significant increase in global firing rate of putative VTA dopaminergic neurons (pDAergic) (Fig. 4E; F(2,56)=17.6, p<0.000, one-way ANOVA), with an average spike latency of 170ms (Fig. 4-1A), indicative of polysynaptic modulation.

Of these pDAergic neurons, 82.8% increased activity during stimulation (Fig. 4F-G). No significant differences were observed in the activity of putative GABAergic VTA neurons, though there was a trend for decreased activity during D2-MSN stimulation (Fig. 4E-G).

The previous data suggested an indirect modulation of VTA activity through the VP, so we decided to optogenetically stimulate D2-MSN terminals in the VP during the PR test (Fig. 4H-K). Regarding training, both groups learned in a similar manner (CRF: Fig. 4-1B; $F(1,72)=0.0$, $p=0.856$, 2way ANOVA) (FR: Fig. 4-1C; $F(3,24)=180.4$, $p<0.000$, 2way ANOVA).

Optical stimulation (40 light pulses of 12.5ms at 40Hz) of D2-MSN-VP terminals elicited a significant increase in the breakpoint of ChR2 stimulated rats in comparison with control stimulated rats (40% increase; Fig. 4I; $t(11)=10.7$, $p<0.000$, unpaired t-test). All D2-ChR2 NAc-VP rats displayed a significant increase in breakpoint in the session with optical stimulation (ON) in comparison with the OFF session (Fig. 4J; $t(6)=10.2$, $p<0.000$, paired t-test). No differences in the number of food pellets earned during the PR session was found (Fig. 4K; $t(12)=1.7$, $p=0.112$, unpaired t-test).

Discussion

Local microcircuits in combination with excitatory and inhibitory inputs from upstream regions play an important role in striatal function. Here, we show that activation of D2-MSNs during cue exposure increases willingness to work in the PR test, and that a concerted action of different neurotransmitter systems in the striatum is required for this behavioral effect (Fig. 5).

We first evaluated the impact of GABAergic transmission since GABAergic MSNs highly synapse within each other in the NAc (Dobbs et al., 2016; Sesack and Pickel, 1990), providing a weak lateral inhibitory network (feedback inhibition) (Tepper et al., 2008). This MSN-MSN reciprocal regulation mainly occurs in a $GABA_A$ receptor mediated manner (Tunstall et al., 2002). Our results suggest that the D2-MSN-driven enhancement in motivation is not dependent on GABAergic signalling, since neither $GABA_A$ nor $GABA_B$

525 antagonists normalized the phenotype. However, we do observe an additional increase in
526 the breakpoint of both control and D2-MSN stimulated animals upon $GABA_B$ antagonist
527 administration in the NAc. Such finding is likely to rely on enhanced corticostriatal
528 glutamatergic release upon the blockade of presynaptic $GABA_B$ receptors. In fact, MSNs
529 express $GABA_B$ receptors, application of exogenous $GABA_B$ agonists does not lead to any
530 MSN electrophysiological effect (Logie et al., 2013), though it significantly supresses
531 glutamatergic inputs onto MSNs via a pre-synaptic mechanism (Logie et al., 2013;
532 Nisenbaum et al., 1993). Apart from classic studies showing that NAc cue-evoked firing is
533 abolished by VTA inactivation (Yun et al., 2004), there is also evidence that cue-evoked
534 excitations of NAc core neurons depend on mPFC glutamatergic projections, and contribute
535 to the behavioral response to reward-predictive cues (Ishikawa et al., 2008).

536 Yet, it is important to refer that although sparse, GABAergic interneurons (which do not
537 express D2R) (Tritsch and Sabatini, 2012) display highly branched dendritic and extensive
538 axonal arborisations (English et al., 2012; Ibáñez-Sandoval et al., 2011; Kawaguchi, 1997)
539 and are capable of exerting a powerful control over striatal excitability (feed-forward
540 inhibition) (Tepper et al., 2008, 2004). They also express $GABA_B$ receptors (Logie et al.,
541 2013), so the blockage of this specific feed-forward inhibition might also contribute for the
542 observed increase in motivational drive.

543 In addition to local GABA control, the striatum also contains CINs, which have both
544 excitatory and inhibitory effects in striatal MSNs (Pakhotin and Bracci, 2007; Sullivan and
545 Brake, 2003; Witten et al., 2010). In primates, CINs exhibit multiphasic responses to
546 motivationally salient stimuli that mirror those of midbrain dopamine neurons, being
547 important for reward-related learning (Cachope et al., 2012; Joshua et al., 2008; Kitabatake
548 et al., 2003; Witten et al., 2010). Since 80% of CINs express D2R (Alcantara et al., 2003),
549 one can argue that our optogenetic stimulation protocol directly activates these interneurons,
550 enhancing acetylcholine release in the striatum. In line with this, we found an increase in
551 $ChAT^+/c\text{-}fos^+$ neurons in stimulated animals.

In vivo selective activation of CINs is sufficient to elicit dopamine release directly in the NAc and independently of the soma, by activation of nAChRs in VTA terminals (Cachope et al., 2012; Threlfell et al., 2012). It has been suggested that these nAChR act as dynamic detectors of acetylcholine concentrations, enhancing the contrast between tonic and burst dopaminergic firing (Brunzell et al., 2009). In an elegant study using different KO strains, Champtiaux and colleagues proposed that a combination of α6β2* and α4β2* nAChRs mediate endogenous cholinergic modulation of dopamine release at the VTA terminal level (Champtiaux et al., 2003). Here, we show that α4 antagonist, DHβE, blocks D2-MSN-dependent increase in motivation, suggesting that acetylcholine-mediated dopamine release from VTA terminals is crucial for the observed behavioural effect. It is important to refer that besides CINs, the NAc may also receive cholinergic inputs from the laterodorsal tegmentum (Dautan et al., 2014), though the function of these projections remains completely unknown.

In the NAc, α4 nAChRs subunits are expressed mainly in VTA dopaminergic terminals, but also in some GABAergic fast spiking interneurons (FSI). So, the observed dampening of motivation with α4 antagonist could also depend on these interneurons. However, our data does not support this because GABA receptor antagonists did not abolish the optogenetic-induced behavioural effect.

In addition to local cholinergic control, our data suggests an indirect effect in VTA dopaminergic activity through the VP. First, c-fos analysis revealed increased recruitment of both VP and VTA regions. VP data is somehow surprising considering the GABAergic nature of accumbal-VP monosynaptic projections (Kupchik et al., 2015; Root et al., 2010). Though most studies associate c-fos expression with increased neuronal activity, at least one study has shown that activating striatal MSNs increases c-fos in the VP (Page and Everitt, 1993). Yet, rather than directly associate D2-MSN activation with this increase in c-fos in the VP, we just aim to illustrate that the VP is being differently recruited in stimulated animals. In fact, animals were sacrificed 90 min after the beginning of the PR test, so c-fos reactivity is a sum of all neuronal events that occur during the test, and do not reflect only the optogenetic activation period.

D2-MSN stimulation decreased VP firing rate, and indirectly increased VTA dopaminergic activity, with less effects in GABAergic VTA neurons, consistent with the preferential innervation of VTA dopaminergic neurons by VP inputs (Mahler et al., 2014). So, our hypothesis is that D2-MSNs reduce the tonic VP-VTA inhibitory input, contributing for enhanced dopaminergic activity, which is known to boost motivational drive (Cagniard et al., 2006; Peciña et al., 2003). In fact, it was shown that inhibition of NAc afferents to the VP or direct infusion of GABAergic agonists into the VP, selectively increased the population activity of dopamine neurons, rising NAc dopamine efflux (Floresco et al., 2003). In line with this, we showed that optogenetic activation of D2-MSNs terminals in the VP was sufficient to increase motivation. These findings are in agreement with the emerging notion that the VP is crucial for reward and motivation towards natural rewards and drugs of abuse. In fact, different subregions of the VP mediate different aspects of rewarded behavior, from motivation/incentive salience to reward prediction and consumption (Root et al., 2015; Smith et al., 2009). Yet, it is important to refer that VP is not only a relay area for indirect NAc inputs, since VP neuron responses can occur at a shorter latency than cue-elicited responses in NAc neurons (Richard et al., 2016), and that VP firing rate reflects the strength of incentive motivation (Ahrens et al., 2016).

The increased dopaminergic signals arising from the VTA act mainly (not exclusively since some interneurons also express dopamine receptors) on MSNs either by activating D1R or D2R. Local administration of either D1R or D2R antagonists decreases motivation in control animals, and also abolished D2-MSN-induced positive effects in motivation, indicating a synergistic effect of both MSNs populations. In this perspective, it is important to refer that blockade of D2R would be expected to enhance activity of D2-MSNs since D2Rs are coupled to inhibitory G-proteins (Beaulieu and Gainetdinov, 2011). Yet, one has to bear in mind that D2R antagonists can also act in D2 auto-receptors in VTA terminals, disinhibiting presynaptic control of dopamine release (Anzalone et al., 2012).

Interestingly, D2-MSN optogenetic activation during cue exposure also indirectly recruited D1-MSNs, as assessed by an increase in the number of $D1^{+}$/c-fos^{+} cells in the NAc

upon stimulation. Considering the proposed role for D1R-expressing neurons in reinforcement (Kravitz et al., 2012; Lobo et al., 2010), this activation probably also contributes for the behavioral output.

In summary, we show that NAc D2-MSN optogenetic activation enhances motivation through enhanced VTA-driven dopaminergic signalling. The behavioural effect was dependent on both D1R and D2R signalling in the NAc, suggesting that a coordinated action between these two striatal populations is needed to increase motivational levels.

References

Ahrens AM, Meyer PJ, Ferguson LM, Robinson TE, Aldridge JW (2016) Neural Activity in the Ventral Pallidum Encodes Variation in the Incentive Value of a Reward Cue. J Neurosci 36:7957–7970.

Alcantara AA, Chen V, Herring BE, Mendenhall JM, Berlanga ML (2003) Localization of dopamine D2 receptors on cholinergic interneurons of the dorsal striatum and nucleus accumbens of the rat. Brain Res 986:22–29.

Anzalone A, Lizardi-Ortiz JE, Ramos M, De Mei C, Hopf FW, Iaccarino C, Halbout B, Jacobsen J, Kinoshita C, Welter M, Caron MG, Bonci A, Sulzer D, Borrelli E (2012) Dual Control of Dopamine Synthesis and Release by Presynaptic and Postsynaptic Dopamine D2 Receptors. J Neurosci 32:9023–9034.

Bailey MR, Simpson EH, Balsam PD (2016) Neural substrates underlying effort, time, and risk-based decision making in motivated behavior. Neurobiol Learn Mem 133:233–256.

Basu S, Sarkar C, Chakroborty D, Nagy J, Mitra RB, Dasgupta PS, Mukhopadhyay D (2004) Ablation of Peripheral Dopaminergic Nerves Stimulates Malignant Tumor Growth by Inducing Vascular Permeability Factor/Vascular Endothelial Growth Factor-Mediated Angiogenesis. Cancer Res 64:5551–5555.

Beaulieu J-M, Gainetdinov RR (2011) The physiology, signaling, and pharmacology of dopamine receptors. Pharmacol Rev 63:182–217.

Bocklisch C, Pascoli V, Wong JCY, House DRC, Yvon C, de Roo M, Tan KR, Lüscher C (2013) Cocaine disinhibits dopamine neurons by potentiation of GABA transmission in the ventral tegmental area. Science 341:1521–1525.

Brunzell DH, Boschen KE, Hendrick ES, Beardsley PM, McIntosh JM (2009) α-Conotoxin MII-Sensitive Nicotinic Acetylcholine Receptors in the Nucleus Accumbens Shell Regulate Progressive Ratio Responding Maintained by Nicotine. Neuropsychopharmacology 35:665–673.

Cachope R, Mateo Y, Mathur BN, Irving J, Wang H-L, Morales M, Lovinger DM, Cheer JF (2012) Selective Activation of Cholinergic Interneurons Enhances Accumbal Phasic Dopamine Release: Setting the Tone for Reward Processing. Cell Rep 2:33–41.

Cagniard B, Balsam PD, Brunner D, Zhuang X (2006) Mice with chronically elevated dopamine exhibit enhanced motivation, but not learning, for a food reward. Neuropsychopharmacol Off Publ Am Coll Neuropsychopharmacol 31:1362–1370.

Champtiaux N, Gotti C, Cordero-Erausquin M, David DJ, Przybylski C, Léna C, Clementi F, Moretti M, Rossi FM, Le Novère N, McIntosh JM, Gardier AM, Changeux J-P (2003) Subunit composition of functional nicotinic receptors in dopaminergic neurons investigated with knock-out mice. J Neurosci Off J Soc Neurosci 23:7820–7829.

654 Creed M, Ntamati NR, Chandra R, Lobo MK, Lüscher C (2016) Convergence of Reinforcing and
655 Anhedonic Cocaine Effects in the Ventral Pallidum. Neuron 92:214–226.
656 Dautan D, Huerta-Ocampo I, Witten IB, Deisseroth K, Bolam JP, Gerdjikov T, Mena-Segovia J (2014)
657 A major external source of cholinergic innervation of the striatum and nucleus accumbens
658 originates in the brainstem. J Neurosci Off J Soc Neurosci 34:4509–4518.
659 Dobbs LK, Kaplan AR, Lemos JC, Matsui A, Rubinstein M, Alvarez VA (2016) Dopamine Regulation
660 of Lateral Inhibition between Striatal Neurons Gates the Stimulant Actions of Cocaine. Neuron
661 90:1100–1113.
662 English DF, Ibanez-Sandoval O, Stark E, Tecuapetla F, Buzsáki G, Deisseroth K, Tepper JM, Koos T
663 (2012) GABAergic circuits mediate the reinforcement-related signals of striatal cholinergic
664 interneurons. Nat Neurosci 15:123–130.
665 Floresco SB, West AR, Ash B, Moore H, Grace AA (2003) Afferent modulation of dopamine neuron
666 firing differentially regulates tonic and phasic dopamine transmission. Nat Neurosci 6:968–
667 973.
668 Gerfen CR (1984) The neostriatal mosaic: compartmentalization of corticostriatal input and
669 striatonigral output systems. Nature 311:461–464.
670 Giorgetti M, Hotsenpiller G, Froestl W, Wolf ME (2002) In vivo modulation of ventral tegmental area
671 dopamine and glutamate efflux by local GABAB receptors is altered after repeated
672 amphetamine treatment. Neuroscience 109:585–595.
673 Grace AA, Floresco SB, Goto Y, Lodge DJ (2007) Regulation of firing of dopaminergic neurons and
674 control of goal-directed behaviors. Trends Neurosci 30:220–227.
675 Haber SN (2003) The primate basal ganglia: parallel and integrative networks. J Chem Neuroanat
676 26:317–330.
677 Hill JA, Zoli M, Bourgeois JP, Changeux JP (1993) Immunocytochemical localization of a neuronal
678 nicotinic receptor: the beta 2-subunit. J Neurosci 13:1551–1568.
679 Hjelmstad GO, Xia Y, Margolis EB, Fields HL (2013) Opioid Modulation of Ventral Pallidal Afferents to
680 Ventral Tegmental Area Neurons. J Neurosci 33:6454–6459.
681 Hyman SE, Malenka RC, Nestler EJ (2006) NEURAL MECHANISMS OF ADDICTION: The Role of
682 Reward-Related Learning and Memory. Annu Rev Neurosci 29:565–598.
683 Ibáñez-Sandoval O, Tecuapetla F, Unal B, Shah F, Koós T, Tepper JM (2011) A novel functionally
684 distinct subtype of striatal neuropeptide Y interneuron. J Neurosci Off J Soc Neurosci
685 31:16757–16769.
686 Ibáñez-Sandoval O, Tecuapetla F, Unal B, Shah F, Koós T, Tepper JM (2010) Electrophysiological
687 and morphological characteristics and synaptic connectivity of tyrosine hydroxylase-
688 expressing neurons in adult mouse striatum. J Neurosci Off J Soc Neurosci 30:6999–7016.
689 Ibáñez-Sandoval O, Xenias HS, Tepper JM, Koós T (2015) Dopaminergic and cholinergic modulation
690 of striatal tyrosine hydroxylase interneurons. Neuropharmacology 95:468–476.
691 Ikeda H, Kotani A, Koshikawa N, Cools AR (2010) Differential role of GABAA and GABAB receptors
692 in two distinct output stations of the rat striatum: studies on the substantia nigra pars
693 reticulata and the globus pallidus. Neuroscience 167:31–39.
694 Ishikawa A, Ambroggi F, Nicola SM, Fields HL (2008) Dorsomedial Prefrontal Cortex Contribution to
695 Behavioral and Nucleus Accumbens Neuronal Responses to Incentive Cues. J Neurosci
696 28:5088–5098.
697 Jin X, Tecuapetla F, Costa RM (2014) Basal ganglia subcircuits distinctively encode the parsing and
698 concatenation of action sequences. Nat Neurosci 17:423–430.
699 Jones IW, Bolam JP, Wonnacott S (2001) Presynaptic localisation of the nicotinic acetylcholine
700 receptor β2 subunit immunoreactivity in rat nigrostriatal dopaminergic neurones. J Comp
701 Neurol 439:235–247.
702 Jones IW, Wonnacott S (2004) Precise Localization of α7 Nicotinic Acetylcholine Receptors on
703 Glutamatergic Axon Terminals in the Rat Ventral Tegmental Area. J Neurosci 24:11244–
704 11252.
705 Joshua M, Adler A, Mitelman R, Vaadia E, Bergman H (2008) Midbrain dopaminergic neurons and
706 striatal cholinergic interneurons encode the difference between reward and aversive events at
707 different epochs of probabilistic classical conditioning trials. J Neurosci Off J Soc Neurosci
708 28:11673–11684.
709 Kandov Y, Israel Y, Kest A, Dostova I, Verasammy J, Bernal SY, Kasselman L, Bodnar RJ (2006)
710 GABA receptor subtype antagonists in the nucleus accumbens shell and ventral tegmental
711 area differentially alter feeding responses induced by deprivation, glucoprivation and
712 lipoprivation in rats. Brain Res 1082:86–97.
713 Kawaguchi Y (1997) Neostriatal cell subtypes and their functional roles. Neurosci Res 27:1–8.

Kelley AE, Berridge KC (2002) The Neuroscience of Natural Rewards: Relevance to Addictive Drugs. J Neurosci 22:3306–3311.

Kitabatake Y, Hikida T, Watanabe D, Pastan I, Nakanishi S (2003) Impairment of reward-related learning by cholinergic cell ablation in the striatum. Proc Natl Acad Sci 100:7965–7970.

Koós T, Tepper JM (1999) Inhibitory control of neostriatal projection neurons by GABAergic interneurons. Nat Neurosci 2:467–472.

Kravitz AV, Tye LD, Kreitzer AC (2012) Distinct roles for direct and indirect pathway striatal neurons in reinforcement. Nat Neurosci 15:816–818.

Kupchik YM, Brown RM, Heinsbroek JA, Lobo MK, Schwartz DJ, Kalivas PW (2015) Coding the direct/indirect pathways by D1 and D2 receptors is not valid for accumbens projections. Nat Neurosci advance online publication.

Lim SAO, Kang UJ, McGehee DS (2014) Striatal cholinergic interneuron regulation and circuit effects. Front Synaptic Neurosci 6.

Lobo MK, Covington HE, Chaudhury D, Friedman AK, Sun H, Damez-Werno D, Dietz DM, Zaman S, Koo JW, Kennedy PJ, Mouzon E, Mogri M, Neve RL, Deisseroth K, Han M-H, Nestler EJ (2010) Cell Type–Specific Loss of BDNF Signaling Mimics Optogenetic Control of Cocaine Reward. Science 330:385–390.

Löf E, Olausson P, deBejczy A, Stomberg R, McIntosh JM, Taylor JR, Söderpalm B (2007) Nicotinic acetylcholine receptors in the ventral tegmental area mediate the dopamine activating and reinforcing properties of ethanol cues. Psychopharmacology (Berl) 195:333–343.

Logie C, Bagetta V, Bracci E (2013) Presynaptic Control of Corticostriatal Synapses by Endogenous GABA. J Neurosci 33:15425–15431.

Lu XY, Ghasemzadeh MB, Kalivas PW (1998) Expression of D1 receptor, D2 receptor, substance P and enkephalin messenger RNAs in the neurons projecting from the nucleus accumbens. Neuroscience 82:767–780.

Luedtke RR, Griffin SA, Conroy SS, Jin X, Pinto A, Sesack SR (1999) Immunoblot and immunohistochemical comparison of murine monoclonal antibodies specific for the rat D1a and D1b dopamine receptor subtypes. J Neuroimmunol 101:170–187.

Luessen DJ, Hinshaw TP, Sun H, Howlett AC, Marrs G, McCool BA, Chen R (2016) RGS2 modulates the activity and internalization of dopamine D2 receptors in neuroblastoma N2A cells. Neuropharmacology 110:297–307.

Mahler SV, Vazey EM, Beckley JT, Keistler CR, McGlinchey EM, Kaufling J, Wilson SP, Deisseroth K, Woodward JJ, Aston-Jones G (2014) Designer receptors show role for ventral pallidum input to ventral tegmental area in cocaine seeking. Nat Neurosci 17:577–585.

Nadal R, Armario A, Janak P (2002) Positive relationship between activity in a novel environment and operant ethanol self-administration in rats. Psychopharmacology (Berl) 162:333–338.

Natsubori A, Tsutsui-Kimura I, Nishida H, Bouchekioua Y, Sekiya H, Uchigashima M, Watanabe M, de Kerchove d'Exaerde A, Mimura M, Takata N, Tanaka KF (2017) Ventrolateral Striatal Medium Spiny Neurons Positively Regulate Food-Incentive, Goal-Directed Behavior Independently of D1 and D2 Selectivity. J Neurosci Off J Soc Neurosci 37:2723–2733.

Nicklas W, Baneux P, Boot R, Decelle T, Deeny AA, Fumanelli M, Illgen-Wilcke B, FELASA (Federation of European Laboratory Animal Science Associations Working Group on Health Monitoring of Rodent and Rabbit Colonies) (2002) Recommendations for the health monitoring of rodent and rabbit colonies in breeding and experimental units. Lab Anim 36:20–42.

Nisenbaum ES, Berger TW, Grace AA (1993) Depression of glutamatergic and GABAergic synaptic responses in striatal spiny neurons by stimulation of presynaptic GABAB receptors. Synap N Y N 14:221–242.

Page KJ, Everitt BJ (1993) Transsynaptic induction of c-fos in basal forebrain, diencephalic and midbrain neurons following AMPA-induced activation of the dorsal and ventral striatum. Exp Brain Res 93:399–411.

Pakhotin P, Bracci E (2007) Cholinergic interneurons control the excitatory input to the striatum. J Neurosci Off J Soc Neurosci 27:391–400.

Paxinos G, Watson C (2005) The Rat Brain in Stereotaxic Coordinates. Elsevier Academic Press.

Peciña S, Cagniard B, Berridge KC, Aldridge JW, Zhuang X (2003) Hyperdopaminergic mutant mice have higher "wanting" but not "liking" for sweet rewards. J Neurosci Off J Soc Neurosci 23:9395–9402.

Perry ML, Pratt WE, Baldo BA (2014) Overlapping striatal sites mediate scopolamine-induced feeding suppression and mu-opioid-mediated hyperphagia in the rat. Psychopharmacology (Berl) 231:919–928.

774 Rahman S, McBride WJ (2002) Involvement of GABA and cholinergic receptors in the nucleus
775 accumbens on feedback control of somatodendritic dopamine release in the ventral tegmental
776 area. J Neurochem 80:646–654.
777 Rice ME, Cragg SJ (2004) Nicotine amplifies reward-related dopamine signals in striatum. Nat
778 Neurosci 7:583–584.
779 Richard JM, Ambroggi F, Janak PH, Fields HL (2016) Ventral Pallidum Neurons Encode Incentive
780 Value and Promote Cue-Elicited Instrumental Actions. Neuron 90:1165–1173.
781 Root DH, Fabbricatore AT, Ma S, Barker DJ, West MO (2010) Rapid phasic activity of ventral pallidal
782 neurons during cocaine self-administration. Synap N Y N 64:704–713.
783 Root DH, Melendez RI, Zaborszky L, Napier TC (2015) The ventral pallidum: Subregion-specific
784 functional anatomy and roles in motivated behaviors. Prog Neurobiol 130:29–70.
785 Sesack SR, Pickel VM (1990) In the rat medial nucleus accumbens, hippocampal and
786 catecholaminergic terminals converge on spiny neurons and are in apposition to each other.
787 Brain Res 527:266–279.
788 Smith KS, Tindell AJ, Aldridge JW, Berridge KC (2009) Ventral pallidum roles in reward and
789 motivation. Behav Brain Res 196:155–167.
790 Soares-Cunha C, Coimbra B, David-Pereira A, Borges S, Pinto L, Costa P, Sousa N, Rodrigues AJ
791 (2016a) Activation of D2 dopamine receptor-expressing neurons in the nucleus accumbens
792 increases motivation. Nat Commun 7:11829.
793 Soares-Cunha C, Coimbra B, Sousa N, Rodrigues AJ (2016b) Reappraising striatal D1- and D2-
794 neurons in reward and aversion. Neurosci Biobehav Rev 68:370–386.
795 Sullivan RM, Brake WG (2003) What the rodent prefrontal cortex can teach us about attention-
796 deficit/hyperactivity disorder: the critical role of early developmental events on prefrontal
797 function. Behav Brain Res 146:43–55.
798 Tepper JM, Bolam JP (2004) Functional diversity and specificity of neostriatal interneurons. Curr Opin
799 Neurobiol 14:685–692.
800 Tepper JM, Koós T, Wilson CJ (2004) GABAergic microcircuits in the neostriatum. Trends Neurosci
801 27:662–669.
802 Tepper JM, Wilson CJ, Koós T (2008) Feedforward and feedback inhibition in neostriatal GABAergic
803 spiny neurons. Brain Res Rev 58:272–281.
804 Threlfell S, Lalic T, Platt NJ, Jennings KA, Deisseroth K, Cragg SJ (2012) Striatal dopamine release is
805 triggered by synchronized activity in cholinergic interneurons. Neuron 75:58–64.
806 Totah NKB, Kim Y, Moghaddam B (2013) Distinct prestimulus and poststimulus activation of VTA
807 neurons correlates with stimulus detection. J Neurophysiol 110:75–85.
808 Tritsch NX, Sabatini BL (2012) Dopaminergic modulation of synaptic transmission in cortex and
809 striatum. Neuron 76:33–50.
810 Tunstall MJ, Oorschot DE, Kean A, Wickens JR (2002) Inhibitory interactions between spiny
811 projection neurons in the rat striatum. J Neurophysiol 88:1263–1269.
812 Ungless MA, Grace AA (2012) Are you or aren't you? Challenges associated with physiologically
813 identifying dopamine neurons. Trends Neurosci 35:422–430.
814 Ungless MA, Magill PJ, Bolam JP (2004) Uniform inhibition of dopamine neurons in the ventral
815 tegmental area by aversive stimuli. Science 303:2040–2042.
816 Vezina P, Blanc G, Glowinski J, Tassin JP (1994) Blockade of D-1 dopamine receptors in the medial
817 prefrontal cortex produces delayed effects on pre- and postsynaptic indices of dopamine
818 function in the nucleus accumbens. Synap N Y N 16:104–112.
819 Vicente AM, Galvão-Ferreira P, Tecuapetla F, Costa RM (2016) Direct and indirect dorsolateral
820 striatum pathways reinforce different action strategies. Curr Biol CB 26:R267-269.
821 Wise RA (2004) Dopamine, learning and motivation. Nat Rev Neurosci 5:483–494.
822 Wise RA (1998) Drug-activation of brain reward pathways. Drug Alcohol Depend 51:13–22.
823 Witten IB, Lin S-C, Brodsky M, Prakash R, Diester I, Anikeeva P, Gradinaru V, Ramakrishnan C,
824 Deisseroth K (2010) Cholinergic interneurons control local circuit activity and cocaine
825 conditioning. Science 330:1677–1681.
826 Wonnacott S, Kaiser S, Mogg A, Soliakov L, Jones IW (2000) Presynaptic nicotinic receptors
827 modulating dopamine release in the rat striatum. Eur J Pharmacol 393:51–58.
828 Wu M, Hrycyshyn AW, Brudzynski SM (1996) Subpallidal outputs to the nucleus accumbens and the
829 ventral tegmental area: anatomical and electrophysiological studies. Brain Res 740:151–161.
830 Yan Z, Flores-Hernandez J, Surmeier DJ (2001) Coordinated expression of muscarinic receptor
831 messenger RNAs in striatal medium spiny neurons. Neuroscience 103:1017–1024.

Yee J, Famous KR, Hopkins TJ, McMullen MC, Pierce RC, Schmidt HD (2011) Muscarinic acetylcholine receptors in the nucleus accumbens core and shell contribute to cocaine priming-induced reinstatement of drug seeking. Eur J Pharmacol 650:596–604.

Yun IA, Wakabayashi KT, Fields HL, Nicola SM (2004) The Ventral Tegmental Area Is Required for the Behavioral and Nucleus Accumbens Neuronal Firing Responses to Incentive Cues. J Neurosci 24:2923–2933.

Zalocusky KA, Ramakrishnan C, Lerner TN, Davidson TJ, Knutson B, Deisseroth K (2016) Nucleus accumbens D2R cells signal prior outcomes and control risky decision-making. Nature 531:642–646.

Zhou L, Furuta T, Kaneko T (2003) Chemical organization of projection neurons in the rat accumbens nucleus and olfactory tubercle. Neuroscience 120:783–798.

Legends to Figures

Fig. 1. Optical stimulation of NAc D2-MSNs increases motivation. ***A***, AAV5-D2-ChR2(H134R)-eYFP (D2-ChR2 group) or AAV5-D2-eYFP (D2-eYFP group) was unilaterally injected in the NAc of Wistar han rats. An hybrid cannula was placed in the NAc to allow simultaneous delivery of fluids and optical stimulation. ***B***, Expression of eYFP was confirmed by YFP immunostaining; scale bar=500µm; numbers represent distance to bregma in mm. ***C***, Representative immunostaining for D2R and eYFP in the NAc of an animal injected with AAV5-D2-ChR2(H134R)-eYFP; scale bar=100µm, inset scale bar=50 µm. More than 50% of D2-MSNs were transfected (n=6 animals/group). ***D***, Upon D2-MSN optical stimulation (12.5ms light pulses at 40Hz, during 1s), 60% of cells increased activity, 16% decreased and 24% did not respond in comparison with baseline (n=25 cells from 4 rats). ***E***, Time histogram of NAc electrophysiological single units in response to optical stimulus (average of 25 cells; blue stripe corresponds to laser stimulation); ***E'***, example of a ChR2 neuron that responds to each pulse of stimulation; right: example of a representative MSN waveform. ***F***, Increase in NAc average firing rate during optogenetic stimulation of D2-MSNs. ***G***, Spike latency in response to D2-MSN optical stimulation. ***H***, Continuous reinforcement (CRF) training sessions of the PR test. ***I***, Fixed ratio (FR) training sessions of the PR test. ***J***, Optogenetic activation of D2-MSNs during cue exposure strongly enhanced breakpoint. ***K***, All animals increase breakpoint in the session with D2-MSN stimulation (ON) versus OFF session. ***L***, Number of pellets consumed in the PR session with stimulation was similar between groups. ***M***, Optogenetic activation of D2-MSNs during inter-trial interval (ITI) does not alter breakpoint. ***N***, Number of pellets earned in the PR session with stimulation on ITI was similar between groups. $n_{D2\text{-}eYFP}$=7; $n_{D2\text{-}ChR2}$=10. Error bars denote SEM. ***p<0.001. *See extended data – Fig. 1-1, 1-2.*

Fig. 2. Effects of different antagonists in motivation. ***A***, Simplified schematic representation of NAc microcircuit. *Left:* The NAc receives cortical (PFC) glutamatergic inputs and VTA dopaminergic inputs. NAc D1- and D2-MSNs send GABAergic projections to ventral pallidum (VP), which in turn projects back to the NAc (not represented) and to VTA (amongst other regions). Besides MSNs, the NAc contains cholinergic interneurons (CIN) and GABAergic interneurons of different natures, including fast spiking interneurons (FSI), which tightly regulate striatal activity. *Right:* expression of different neurotransmitter receptors in striatal neurons and terminals. Of relevance to mention that CINs also express dopamine receptor D2R, and can stimulate dopamine release from VTA terminals mainly in

a $\alpha4\beta2$*nAchR or $\alpha6\beta2$*nAchR-dependent manner. Activation of D2R autoreceptors located in VTA terminals also controls dopamine release. iGluR: ionotropic glutamate receptors; mGluR: metabotropic glutamate receptors; nAchR: nicotinic (ionotropic) cholinergic receptors; M1/M4: muscarinic (metabotropic) cholinergic receptors. ***B-G***, Effects of different receptor antagonists in behavior. Rats were injected in the NAc with a specific antagonist immediately before the PR test with D2-MSN optogenetic activation. ***B***, $GABA_A$ receptor antagonist did not alter breakpoint of control D2-eYFP animals, nor of D2-ChR2-stimulated animals. ***C***, $GABA_B$ receptor antagonist did not alter breakpoint of control animals, but it further increased the breakpoint of D2-ChR2 stimulated animals. ***D***, Injection of mAChR + nAChR antagonist combination abolished the increased breakpoint of D2-ChR2 stimulated animals. This effect is mediated mainly by nAChR since mecamylamine *per se* normalized breakpoint. ***E***, Local administration of α4-nAChR antagonist blocked the effect of D2-MSN optogenetic activation. ***F***, D1R antagonist decreases the breakpoint of control D2-eYFP animals. In addition, the breakpoint enhancement induced by optogenetic activation of D2-MSNs was completely abolished by this treatment. ***G***, D2R antagonist originated a similar effect as D1R antagonist. ***H***, Summary of the effects of different antagonists in the breakpoint of stimulated D2-eYFP and D2-ChR2 animals. ($n_{D2\text{-}eYFP}$ =7; $n_{D2\text{-}ChR2}$=8). Error bars denote SEM. * p<0.05, **p<0.01, *** p<0.001, $^{\#}$ p<0.001 and refers to the comparison D2-eYFP treated vs D2-ChR2 treated. *See extended data – Fig. 2-1, 2-2.*

Fig. 3. Effect of optogenetic activation of D2-MSNs in the NAc and downstream targets. ***A***, Representative immunostaining c-fos and D2R, D1R or ChAT in the NAc; scale bar=80μm; ($n_{D2\text{-}ChR2}$=8; $n_{D2\text{-}eYFP}$=7). ***B***, Counting of $D2R^+$ and $c\text{-}fos^+$ cells in the NAc. D2-MSN stimulation recruits more $D2^+$ neurons in comparison to non-stimulated side (contralateral). Stimulated D2-ChR2 animals present increased number of $D2^+/c\text{-}fos^+$ neurons in comparison to stimulated D2-eYFP animals (control group). ***C***, Counting of $D1R^+$ and $c\text{-}fos^+$ cells in the NAc, showing an increase in $D1^+/c\text{-}fos^+$ in stimulated vs contralateral side (or vs D2-eYFP-stimulated animals). ***D***, Counting of $ChAT^+$ and $c\text{-}fos^+$ cells in the NAc, showing an increase in $ChAT^+/c\text{-}fos^+$ in stimulated vs contralateral side (or vs D2-eYFP-stimulated animals. ***E***, Representative immunostaining for TH and c-fos in the VTA (scale bar=100μm) and ***F***, respective quantification of positive cells. D2-MSN stimulation increases the number of TH^+ neurons in the VTA. ***G***, SN $c\text{-}fos^+$ cells counting showing no effect of stimulation. ***H*** Representative immunostaining for c-fos in the VP (scale bar=500μm, inset=100μm) and ***I***, Stimulated D2-ChR2 animals present increased c-fos staining in the VP comparison to control D2-eYFP animals; interestingly, no significant differences were found between

stimulated vs non-stimulated side. Error bars denote SEM. *p<0.05, **p<0.01, ***p<0.001. *SNc: substantia nigra pars compacta. See extended data – Fig. 3-1.*

Fig. 4. Activation of D2-MSN terminals in the ventral pallidum (VP) increases motivation. ***A,*** Schematic representation of the *in vivo* single-cell electrophysiological recordings with optogenetic manipulation of NAc D2-MSN cell bodies. ***B***, NAc D2-MSN optical stimulation (40 Hz, 12.5 ms pulses for 1s) decrease net firing rate of VP neurons. ***C,*** 93.3% of VP cells decrease firing rate and 6.7% did not respond to stimulation (n=30 cells/4 rats). ***D,*** Time histogram showing the number of events in the VP before, during and after a 40Hz stimulus of NAc D2-MSNs. ***E,*** D2-MSN optical stimulation increase the net firing rate of putative dopaminergic (pDAergic) neurons of the VTA, with no significant changes in the net firing rate of putative GABAergic neurons (pGABAergic) ($n_{pDAergic}$=29 cells/4 rats; $n_{GABAergic}$=5cells/4rats). ***F,*** 82.8% of pDAergic cells increased firing rate in response to stimulation; most of cells returned to baseline activity after the stimulus. pGABAergic neurons presented a majority of inhibitory responses to D2-MSN stimulation. ***G,*** Time histogram showing the number of events in the VTA before, during and after a 40Hz stimulus of NAc D2-MSNs. ***H,*** Strategy used for optogenetic stimulation of D2-MSN terminals in the VP (D2-ChR2 NAc-VP group). ***I***, Optogenetic activation of D2-MSN-VP terminals during cue exposure strongly enhanced breakpoint. ***J***, All animals increase breakpoint in the session with stimulation (ON) vs non-stimulation session (OFF). ***K***, Number of pellets consumed in the PR session was similar between groups. ($n_{D2\text{-}eYFP\ NAc\text{-}VP}$ =6; $n_{D2\text{-}ChR2\ NAc\text{-}VP}$=8). Error bars denote SEM. *** p<0.001. *See extended data – Fig. 4-1.*

Fig. 5. Proposed model for D2-MSN optogenetic activation effects in NAc microcircuit. NAc D2-MSNs send GABAergic projections to VP neurons, which in turn provide a tonic inhibitory input to the VTA. (1) Optogenetic activation of D2-MSNs reduces VP net activity (2), reducing VP-to-VTA inhibitory tone (3). This triggers an increase in VTA dopaminergic activity (4). These VTA dopaminergic signals require D1R and D2R signalling in the NAc (5', 5). Interestingly, cholinergic-dependent control of VTA dopaminergic terminals in the NAc (via α4-nAChR) is essential for this process (6). (7) Optical stimulation can also be activating D2-expressing cholinergic interneurons (CIN) that strongly influence dopamine release and shape behavior.

Legends to Extended Data

Fig. 1-1. Experimental design. ***A***, Animals from Group I were subjected to stereotaxic surgeries for injection of D2-ChR2 or D2-eYFP and optic fiber placement in the nucleus accumbens (NAc), and let to recover from surgery for 2 weeks; after recovering, animals performed the progressive ratio (PR) task. On the PR session day, animals were sacrificed 90 minutes after the beginning of the session for c-fos analysis and immunofluorescence analysis. ***B,*** Animals from Group II were subjected to the same protocol as Group I; one week after performing behavior in naïve conditions, animals were injected in the NAc on one day with the drug and on the other day with vehicle (counterbalanced within groups for treatment between the two test days) before PR performance. This test was repeated for all drugs with one week of interval between treatments. ***C***, Animals from Group III were subjected to stereotaxic surgeries for injection of D2-ChR2 or D2-eYFP in the NAc and optic fiber placement in the ventral pallidum (VP), and performed the PR task as above. ***D***, Animals from Group IV were subjected to the same NAc surgery and were used for *in vivo* single cell electrophysiological recordings in the NAc, VP and VTA.

Fig. 1-2. Confirmation of optic fiber location and expression specificity of Group I. ***A***, Optic fiber placement for D2-eYFP (grey) and D2-ChR2 (blue) rats ($n_{D2\text{-}eYFP}$=7; $n_{D2\text{-}ChR2}$=10). ***B,*** Number of $D2R^+$ and $eYFP^+$ cells per area as evaluated by immunofluorescence. Almost all of $eYFP^+$ cells are also $D2R^+$, confirming the specificity of the construct. ***C,*** Number of $D1R^+$ and $eYFP^+$ cells per area. ***D***, Number of $ChAT^+$ and $eYFP^+$ cells. Only a few $D1R^+$ and $ChAT^+$ cells express the construct ($n_{D2\text{-}eYFP}$=6; $n_{D2\text{-}ChR2}$=6). Error bars denote SEM.

Fig. 2-1. Representative image of viral infection extent and cannula entry site (numbers represent distance to bregma; scale bar=1mm); optic fiber placement for D2-eYFP (grey) and D2-ChR2 (blue) rats of Group II ($n_{D2\text{-}eYFP}$=7; $n_{D2\text{-}ChR2}$=8).

Fig. 2-2. Number of pellets consumed during the PR session with optical stimulation with previous administration of different antagonists. ***A***, $GABA_A$ receptor antagonist (bicuculline, 75ng). ***B***, $GABA_B$ receptor antagonist (GCP-55845, 44ng). ***C***, mAChR antagonist (scopolamine, 25µg) + nAChR antagonist (mecamylamine, 22.5µg). ***D***, α4-nAChR antagonist (DHβE, 0.7µg). ***E***, D1R antagonist (SCH-23390, 0.25µg). ***F***, D2R antagonist (sulpiride, 0.2µg). Error bars denote SEM. *p<0.05.

Fig. 3-1. Immunofluorescence against GFP and dopamine receptor D1 or dopamine receptor D2 in D2-EGFP reporter strain. ***A***, Representative image of a section of a D2-GFP animal labelled with anti-GFP and anti-dopamine receptor D2 (scale bar=50μm). ***B,*** Representative image of a section of a D2-GFP animal labelled with anti-GFP and anti-dopamine receptor D1 (scale bar=50μm). ***C,*** Respective quantification of immunofluorescence. 54.4% of total cells were GFP^+, in agreement with half of the NAc cells being D2-MSNs. Of those GFP^+ cells, 83% were $D2R^+$ and 17% $D2R^-$; whereas most (73%) of these cells were $D1R^-$. Error bars denote SEM.

Fig. 4.1 Additional data from optogenetic activation experiments. ***A***, Spike latency in the VP and VTA neurons in response to NAc D2-MSN optogenetic stimulation. VP neurons present reduced spike latency to fire, consistent with a monosynaptic input from D2-MSNs, whereas VTA neurons present spike latencies indicative of polysynaptic modulation. ***B-C***, CRF and FR learning curves of D2-eYFP and D2-ChR2 NAc-VP animals.

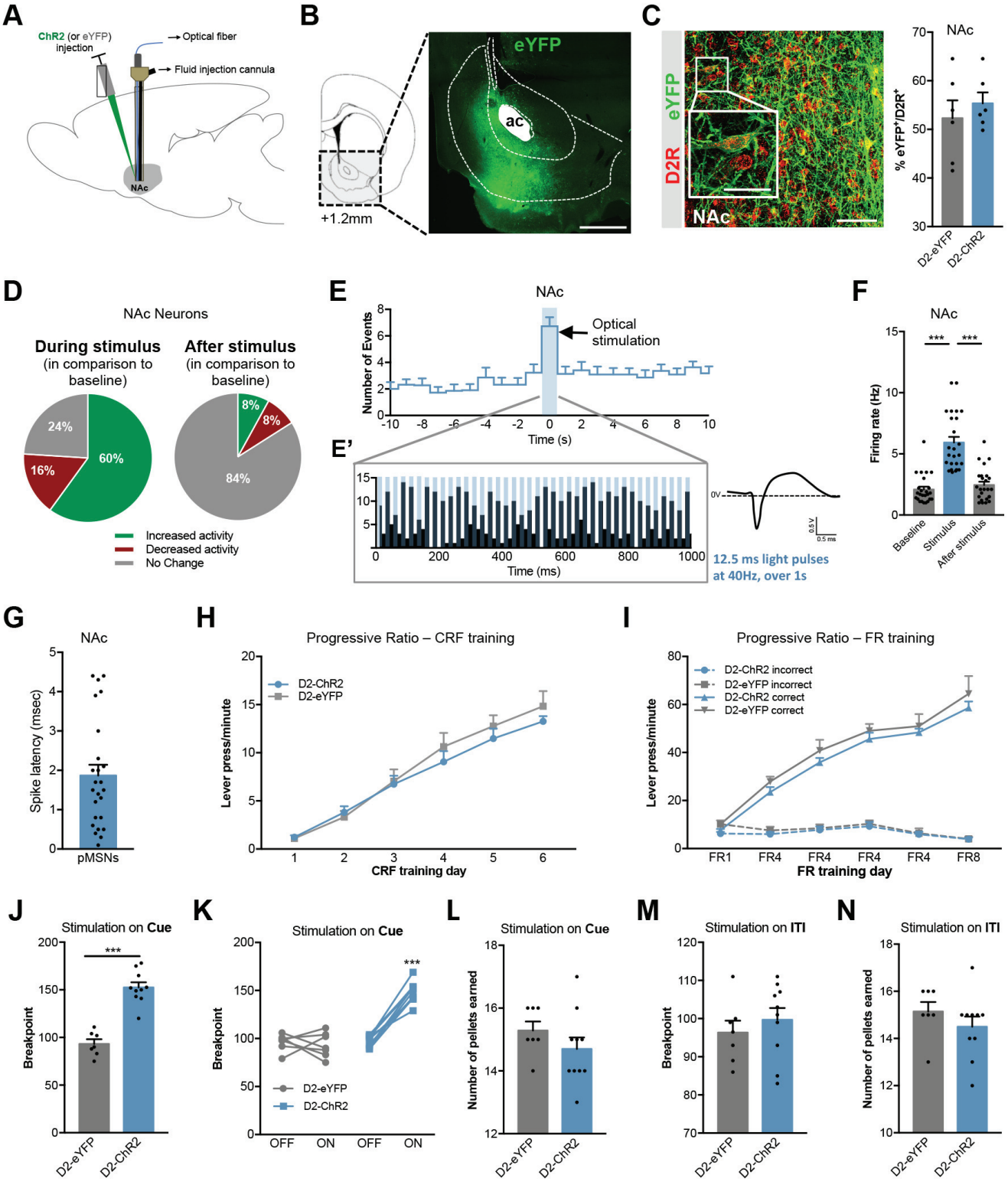

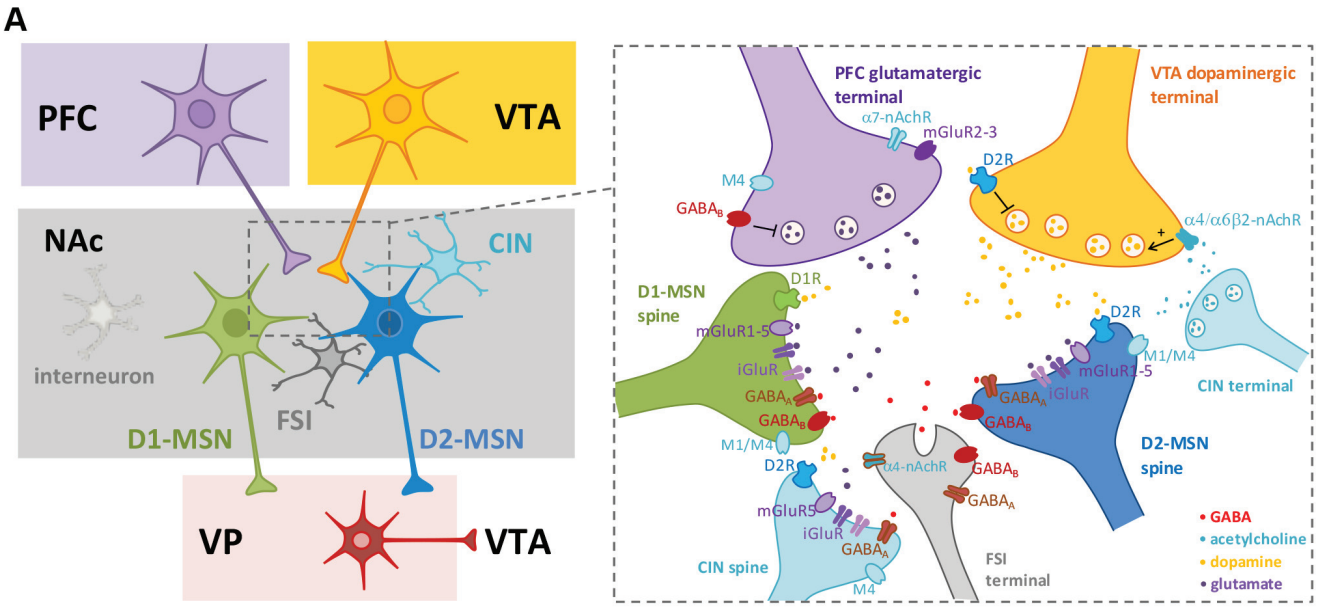

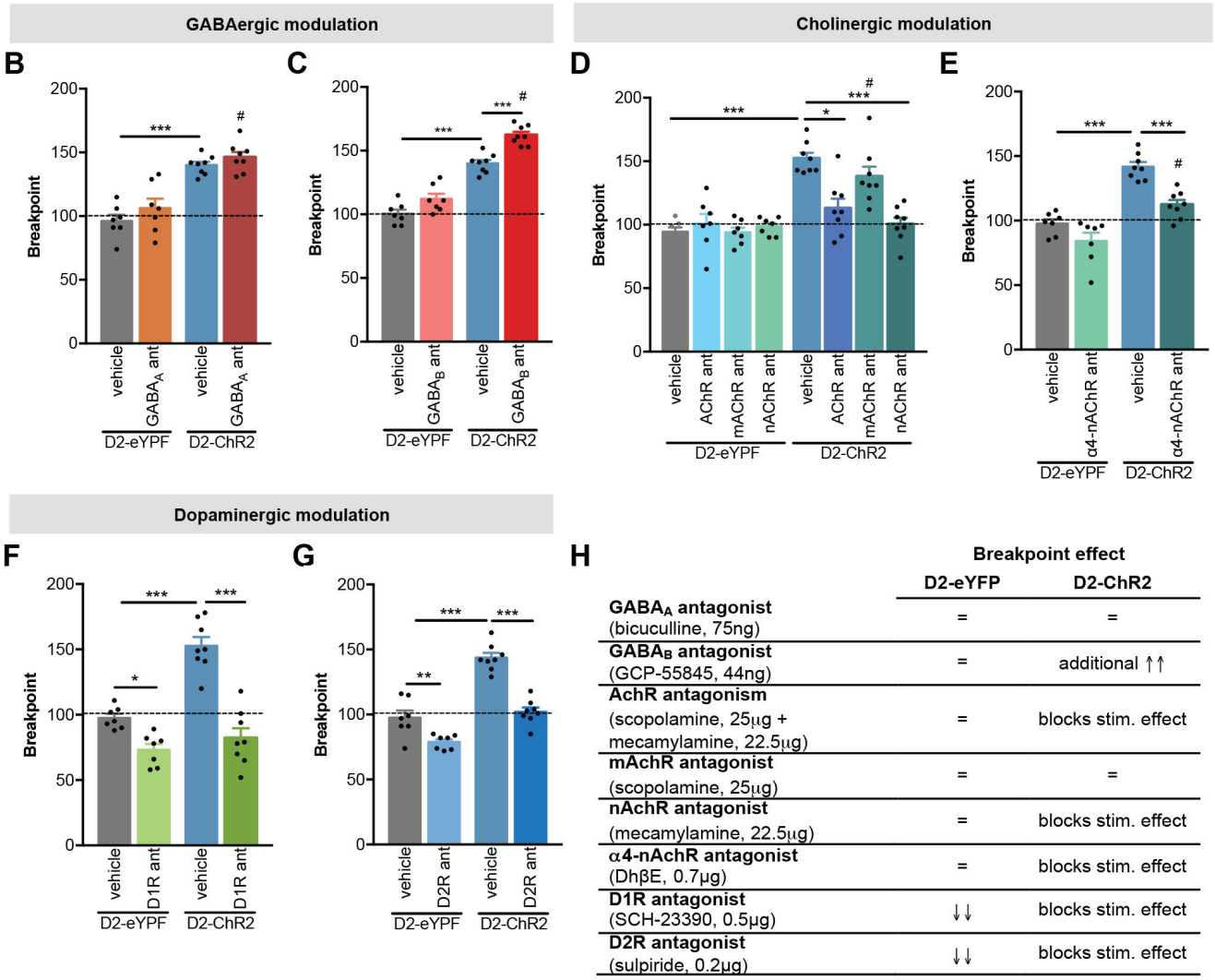

H

	Breakpoint effect	
	D2-eYFP	D2-ChR2
GABA$_A$ antagonist (bicuculline, 75ng)	=	=
GABA$_B$ antagonist (GCP-55845, 44ng)	=	additional ↑↑
AchR antagonism (scopolamine, 25μg + mecamylamine, 22.5μg)	=	blocks stim. effect
mAchR antagonist (scopolamine, 25μg)	=	=
nAchR antagonist (mecamylamine, 22.5μg)	=	blocks stim. effect
α4-nAchR antagonist (DhβE, 0.7μg)	=	blocks stim. effect
D1R antagonist (SCH-23390, 0.5μg)	↓↓	blocks stim. effect
D2R antagonist (sulpiride, 0.2μg)	↓↓	blocks stim. effect

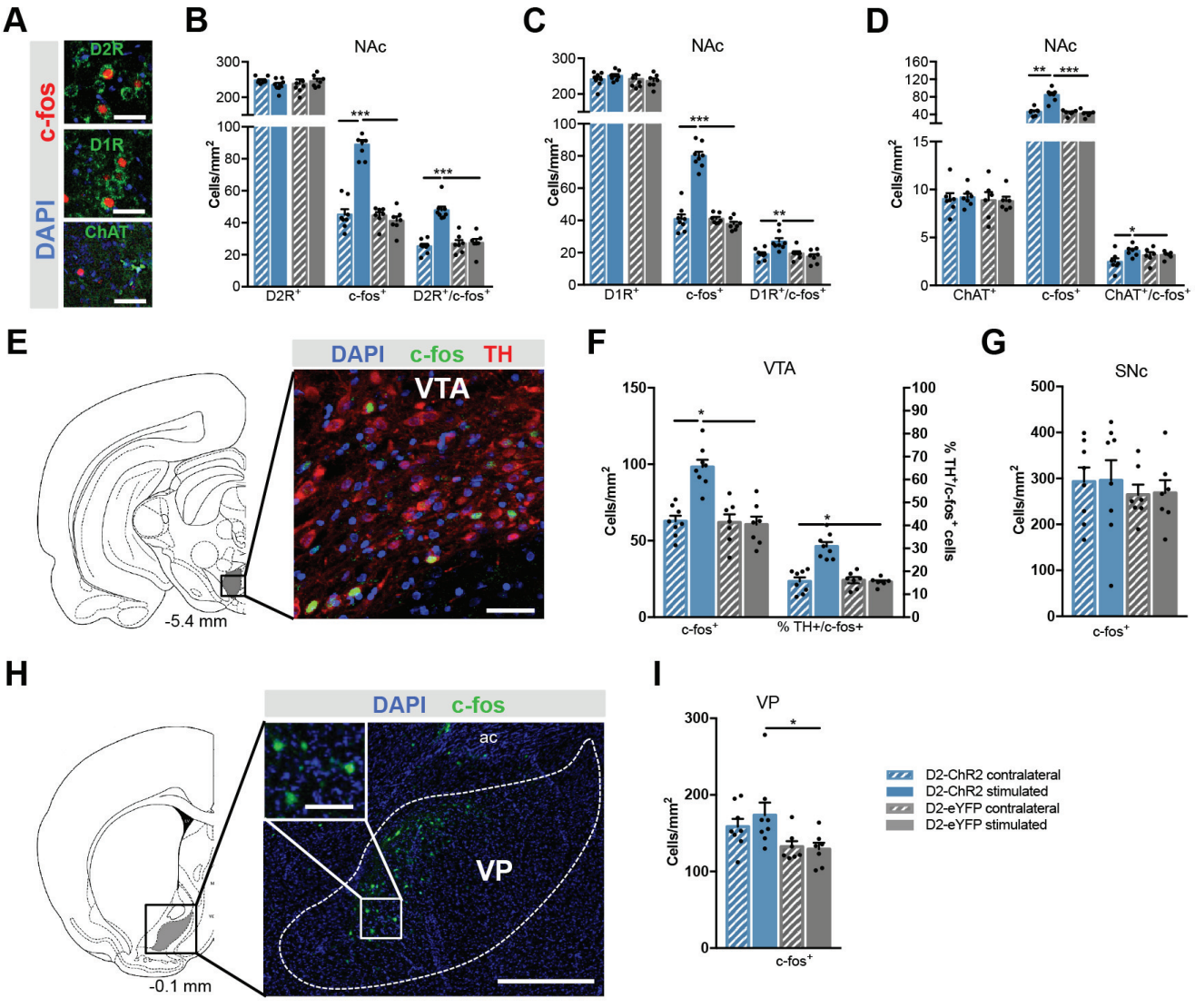

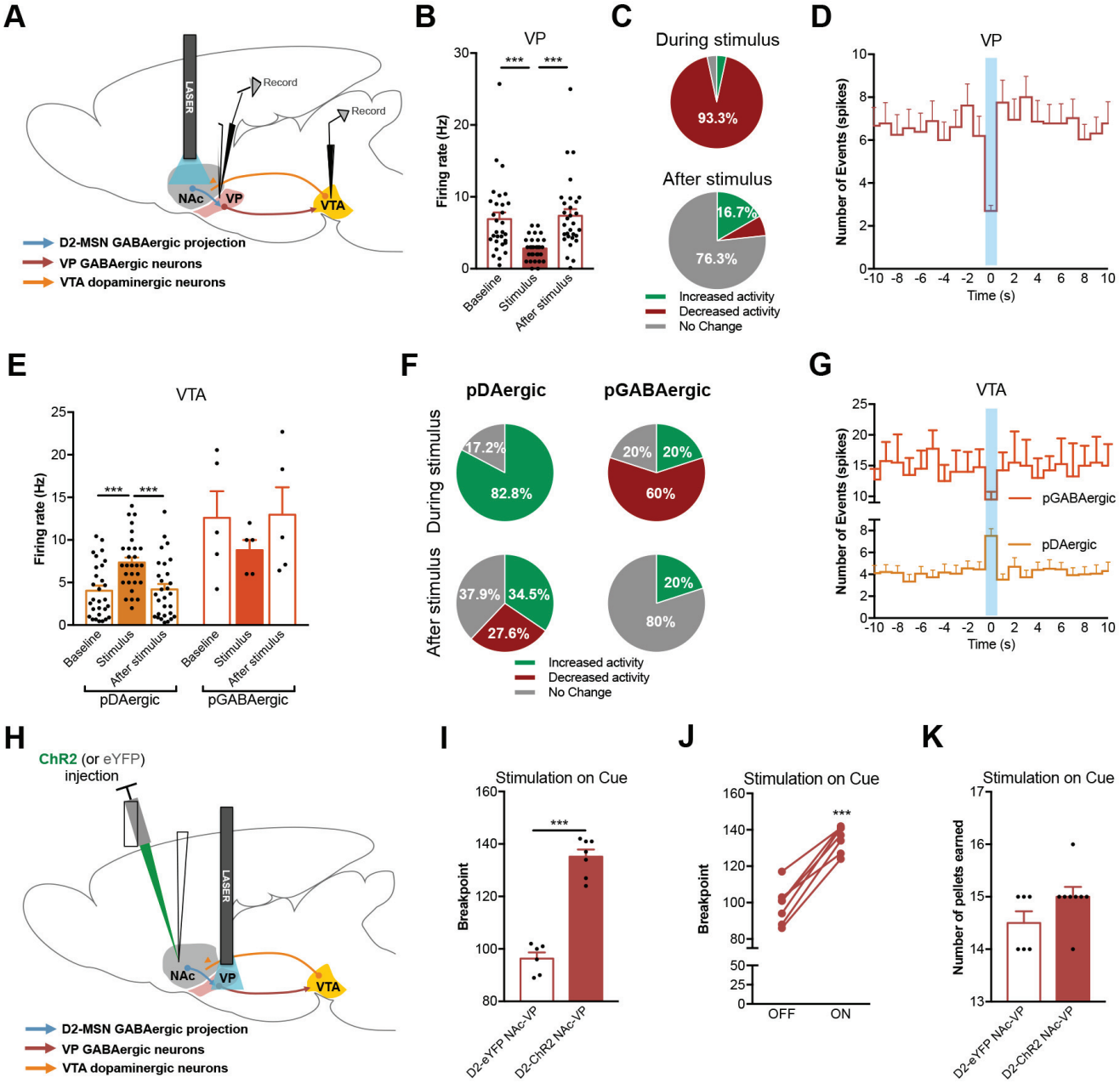

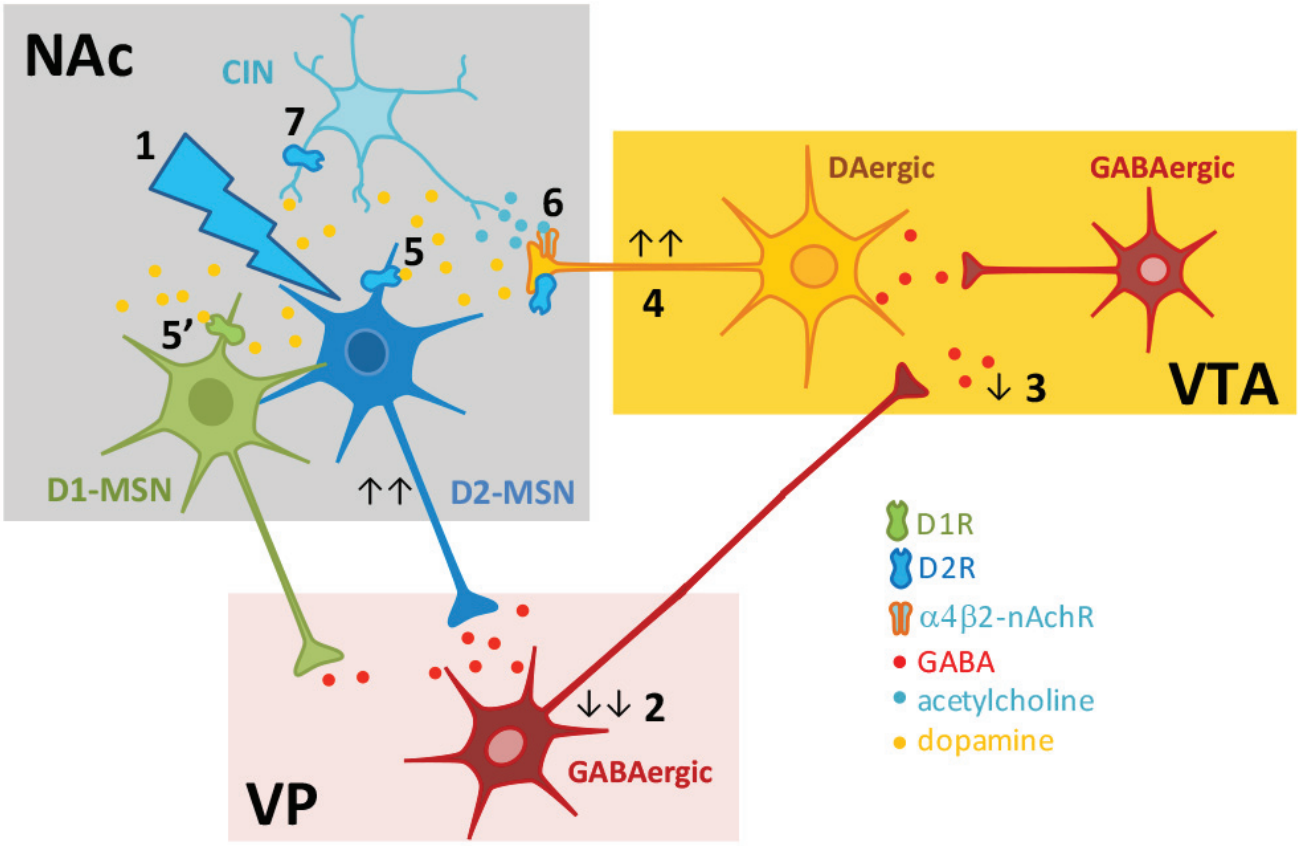

Table 1. Statistical table

Figure	Data Structure	Sample size	Type of Test	Statistics
1F	Normal distribution	23 cells from 4 rats	one-way ANOVA	F(2,48)=74.7, p<0.000
1H	Normal distribution	$n_{D2\text{-}eYFP}$=7; $n_{D2\text{-}ChR2}$=10	2way ANOVA	F(1,13)=0.43, p=0.322
1I	Normal distribution	$n_{D2\text{-}eYFP}$=7; $n_{D2\text{-}ChR2}$=10	2way ANOVA	F(3,30)=124.8, p<0.000
1J	Normal distribution	$n_{D2\text{-}eYFP}$=7; $n_{D2\text{-}ChR2}$=10	Unpaired t-test, tailed	t(13)=7.7, p<0.000
1K	Normal distribution	$n_{D2\text{-}eYFP}$=7; $n_{D2\text{-}ChR2}$=10	2way ANOVA	Laser effect: F(1,13)=47.3, p<0.000 Group effect: F(1,13)=7.9, p<0.000 Bonferroni post test: D2-ChR2 ON vs D2-ChR2 OFF: p<0.001
1L	Normal distribution	$n_{D2\text{-}eYFP}$=7; $n_{D2\text{-}ChR2}$=10	Unpaired t-test, two tailed	t(13)=1.3, p=0.1380
1M	Normal distribution	$n_{D2\text{-}eYFP}$=7; $n_{D2\text{-}ChR2}$=10	Unpaired t-test, two tailed	t(13)=0.7, p=0.4719
1N	Normal distribution	$n_{D2\text{-}eYFP}$=7; $n_{D2\text{-}ChR2}$=10	Unpaired t-test, two tailed	t(13)=1.0, p=0.3124
2B	Normal distribution	$n_{D2\text{-}eYFP\ veh}$=7; $n_{D2\text{-}eYFP\ GABAA\ antag}$=7; $n_{D2\text{-}ChR2\ veh}$=8; $n_{D2\text{-}ChR2\ GABAA\ antag}$=8	2way ANOVA	Treatment effect: F(1,13)=0.1, p=0.117 Group effect: F(1,13)=118.8, p<0.000 Bonferroni post test: D2-ChR2 vehicle vs D2-ChR2 GABA(A) antag: p=0.787
2C	Normal distribution	$n_{D2\text{-}eYFP\ veh}$=7; $n_{D2\text{-}eYFP\ GABAB\ antag}$=7; $n_{D2\text{-}ChR2\ veh}$=8; $n_{D2\text{-}ChR2\ GABAB\ antag}$=8	2way ANOVA	Treatment effect: F(1,13)=30.7, p<0.000 Group effect: F(1,13)=193, p<0.000 Bonferroni post test: D2-eYFP vehicle vs D2-eYFP GABA(B) antag: p=0.07 D2-ChR2 vehicle vs D2-ChR2 GABA(B) antag: p<0.000
2D	Normal distribution	$n_{D2\text{-}eYFP\ veh}$=7; $n_{D2\text{-}eYFP\ mAChR+nAChR\ antag}$=7; $n_{D2\text{-}eYFP\ mAChR\ antag}$=7; $n_{D2\text{-}eYFP\ nAChR\ antag}$=7; $n_{D2\text{-}ChR2\ veh}$=8; $n_{D2\text{-}ChR2\ mAChR+nAChR\ antag}$=8; $n_{D2\text{-}ChR2\ mAChR\ antag}$=8; $n_{D2\text{-}ChR2\ nAChR\ antag}$=8	2way ANOVA	Treatment effect: F(3,39)=4.3, p=0.001 Bonferroni post test: D2-ChR2 vehicle vs D2-ChR2 mAChR+nAChR antag: p<0.000 D2-ChR2 vehicle vs D2-ChR2 nAChR antag: p<0.000
2E	Normal distribution	$n_{D2\text{-}eYFP\ veh}$=7; $n_{D2\text{-}eYFP\ \square4^*\text{-}nAChR\ antag}$=7; $n_{D2\text{-}ChR2\ veh}$=8; $n_{D2\text{-}ChR2\ \square4^*\text{-}nAChR\ antag}$=8	2way ANOVA	Treatment effect: F(1,13)=43.0, p<0.000 Bonferroni post test: D2-ChR2 vehicle vs D2-ChR2 α4 antag: p<0.000

2F	Normal distribution	$n_{D2\text{-}eYFP\ veh}$=7; $n_{D2\text{-}eYFP\ D1R\ antag}$=7; $n_{D2\text{-}ChR2\ veh}$=8; $n_{D2\text{-}ChR2\ D1R\ antag}$=8	2way ANOVA	Treatment effect: D1R antag: F(1,13)=43.7, p<0.000 Bonferroni post test: D2-eYFP vehicle vs D2-eYFP D1R antag: p=0.047 D2-ChR2 vehicle vs D2-ChR2 D1R antag: p<0.000
2G	Normal distribution	$n_{D2\text{-}eYFP\ veh}$=7; $n_{D2\text{-}eYFP\ D2R\ antag}$=7; $n_{D2\text{-}ChR2\ veh}$=8; $n_{D2\text{-}ChR2\ D2R\ antag}$=8	2way ANOVA	Treatment effect: D2R antag: F(1,13)=34.8, p<0.000 Bonferroni post test: D2-eYFP vehicle vs D2-eYFP D2R antag: p=0.013 D2-ChR2 vehicle vs D2-ChR2 D2R antag: p<0.000
3B	Normal distribution	$n_{D2\text{-}ChR2}$=8; $n_{D2\text{-}eYFP}$=7	Unpaired t-test, two tailed	D2-ChR2 vs D2-eYFP rats: t(13)=12.0, p<0.000
3B	Normal distribution	$n_{D2\text{-}ChR2}$=8	Paired t-test, two tailed	Stimulated vs contralateral side: t(7)=7.4, p=0.0002
3C	Normal distribution	$n_{D2\text{-}ChR2}$=8; $n_{D2\text{-}eYFP}$=7	Unpaired t-test, two tailed	D2-ChR2 vs D2-eYFP rats: t(13)=3.7, p=0.0028
3C	Normal distribution	$n_{D2\text{-}ChR2}$=8	Paired t-test, two tailed	Stimulated vs contralateral side: t(7)=3.3, p=0.0011
3D	Normal distribution	$n_{D2\text{-}ChR2}$=8; $n_{D2\text{-}eYFP}$=7	Unpaired t-test, two tailed	D2-ChR2 vs D2-eYFP rats: t(13)=3.7, p<0.000
3D	Normal distribution	$n_{D2\text{-}ChR2}$=8	Paired t-test, two tailed	Stimulated vs contralateral side: t(7)=4.0, p=0.0033
3F	Normal distribution	$n_{D2\text{-}ChR2}$=8; $n_{D2\text{-}eYFP}$=7	Unpaired t-test, two tailed	D2-ChR2 vs D2-eYFP rats: t(13)=3.3, p<0.000
3F	Normal distribution	$n_{D2\text{-}ChR2}$=8	Paired t-test, two tailed	Stimulated vs contralateral side: t(7)=4.4, p=0.0024
3G	Normal distribution	$n_{D2\text{-}ChR2}$=8; $n_{D2\text{-}eYFP}$=7	Unpaired t-test, two tailed	D2-ChR2 vs D2-eYFP rats: t(13)=0.3, p=0.418
3G	Normal distribution	$n_{D2\text{-}ChR2}$=8	Paired t-test, two tailed	Stimulated vs contralateral side: t(7)=0.1, p=0.9099
3I	Normal distribution	$n_{D2\text{-}ChR2}$=8; $n_{D2\text{-}eYFP}$=7	Unpaired t-test, two tailed	D2-ChR2 vs D2-eYFP rats: t(13)=2.3, p=0.039
3I	Normal distribution	$n_{D2\text{-}ChR2}$=8	Paired t-test, two tailed	Stimulated vs contralateral side: t(7)=1.2, p=0.238
4B	Normal distribution	30 cells from 4 rats	one-way ANOVA	F(2,87)=10.4, p<0.000
4E	Normal distribution	29 pDAergic cells from 4 rats 3 pGABAergic cells from 4 rats	one-way ANOVA	pDAergic: F(2,34)=17.4, p<0.000 pGABAergic: F(2,8)=2.7, p=0.1343
4I	Normal	$n_{D2\text{-}ChR2\ NAc\text{-}VP}$=8, $n_{D2\text{-}eYFP\ NAc\text{-}VP}$=4	Unpaired t-test,	t(11)=10.7, p<0.000

	distribution		two tailed	
4J	Normal distribution	$n_{D2\text{-}ChR2\ NAc\text{-}VP}$=8,	Paired t-test, two tailed	t(4)=10.2, p<0.000
4K	Normal distribution	$n_{D2\text{-}ChR2\ NAc\text{-}VP}$=8, $n_{D2\text{-}eYFP\ NAc\text{-}VP}$=4	Unpaired t-test, two tailed	t(12)=1.7, p=0.112
2-2A	Normal distribution	$n_{D2\text{-}eYFP\ veh}$=7; $n_{D2\text{-}eYFP\ GABAA\ antag}$=7; $n_{D2\text{-}ChR2\ veh}$=8; $n_{D2\text{-}ChR2\ GABAA\ antag}$=8	2way ANOVA	Bonferroni post test: D2-eYFP vehicle vs D2-eYFP antag: p=0.4831 D2-ChR2 vehicle vs D2-ChR2 antag: p=0.7434
2-2B	Normal distribution	$n_{D2\text{-}eYFP\ veh}$=7; $n_{D2\text{-}eYFP\ GABAB\ antag}$=7; $n_{D2\text{-}ChR2\ veh}$=8; $n_{D2\text{-}ChR2\ GABAB\ antag}$=8	2way ANOVA	Bonferroni post test: D2-eYFP vehicle vs D2-eYFP antag: p=0.7334 D2-ChR2 vehicle vs D2-ChR2 antag: p=0.9332
2-2C	Normal distribution	$n_{D2\text{-}eYFP\ veh}$=7; $n_{D2\text{-}eYFP\ mAChR+nAChR\ antag}$=7; $n_{D2\text{-}eYFP\ mAChR\ antag}$=7; $n_{D2\text{-}eYFP\ nAChR\ antag}$=7; $n_{D2\text{-}ChR2\ veh}$=8; $n_{D2\text{-}ChR2\ mAChR+nAChR\ antag}$=8; $n_{D2\text{-}ChR2\ mAChR\ antag}$=8; $n_{D2\text{-}ChR2\ nAChR\ antag}$=8	2way ANOVA	Bonferroni post test: D2-eYFP vehicle vs D2-eYFP mAChR+nAChR antag: p=0.9994 D2-ChR2 vehicle vs D2-ChR2 mAChR+nAChR antag: p=0.9883 D2-eYFP vehicle vs D2-eYFP mAChR antag: p=0.9994 D2-ChR2 vehicle vs D2-ChR2 mAChR antag: p=0.9883 D2-eYFP vehicle vs D2-eYFP nAChR antag: p=0.4483 D2-ChR2 vehicle vs D2-ChR2 nAChR antag: p=0.9187
2-2D	Normal distribution	$n_{D2\text{-}eYFP\ veh}$=7; $n_{D2\text{-}eYFP\ \square 4^*\text{-}nAChR\ antag}$=7; $n_{D2\text{-}ChR2\ veh}$=8; $n_{D2\text{-}ChR2\ \square 4^*\text{-}nAChR\ antag}$=8	2way ANOVA	Bonferroni post test: D2-eYFP vehicle vs D2-eYFP antag: p=0.4489 D2-ChR2 vehicle vs D2-ChR2 antag: p=0.7023
2-2E	Normal distribution	$n_{D2\text{-}eYFP\ veh}$=7; $n_{D2\text{-}eYFP\ D1R\ antag}$=7; $n_{D2\text{-}ChR2\ veh}$=8; $n_{D2\text{-}ChR2\ D1R\ antag}$=8	2way ANOVA	Bonferroni post test: D2-eYFP vehicle vs D2-eYFP antag: p=0.0144 D2-ChR2 vehicle vs D2-ChR2 antag: p=0.0842
2-2F	Normal distribution	$n_{D2\text{-}eYFP\ veh}$=7; $n_{D2\text{-}eYFP\ D2R\ antag}$=7; $n_{D2\text{-}ChR2\ veh}$=8; $n_{D2\text{-}ChR2\ D2R\ antag}$=8	2way ANOVA	Bonferroni post test: D2-eYFP vehicle vs D2-eYFP antag: p=0.9999 D2-ChR2 vehicle vs D2-ChR2 antag: p=0.2308
4-1B	Normal distribution	$n_{D2\text{-}ChR2\ NAc\text{-}VP}$=8, $n_{D2\text{-}eYFP\ NAc\text{-}VP}$=6	2way ANOVA	Group effect: F(1,72)=0.0, p=0.856
4-1C	Normal distribution	$n_{D2\text{-}ChR2\ NAc\text{-}VP}$=8, $n_{D2\text{-}eYFP\ NAc\text{-}VP}$=6	2way ANOVA	Day of training effect: F(3,24)=180.4, p<0.000